

# Coarse-Graining Methods in Biology and Materials

---

School on Multiscale Modeling and  
Simulations of Hard and Soft Materials

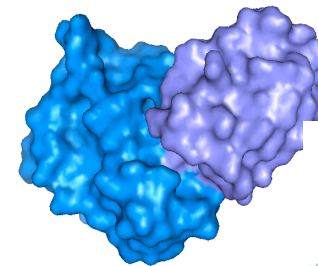
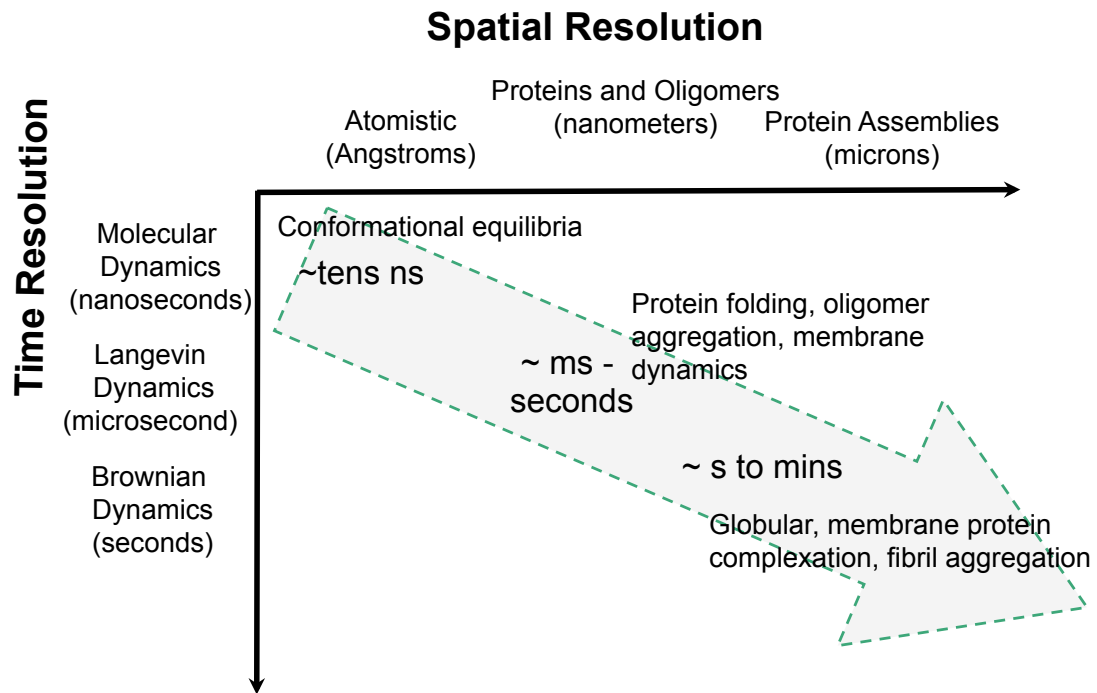
Professor Teresa Head-Gordon  
Department of Bioengineering  
University of California, Berkeley



---

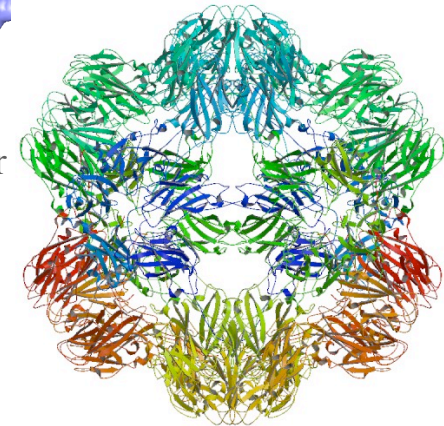
Lecture 2

# Coarse-Graining and MultiScale



Barnase-Barstar

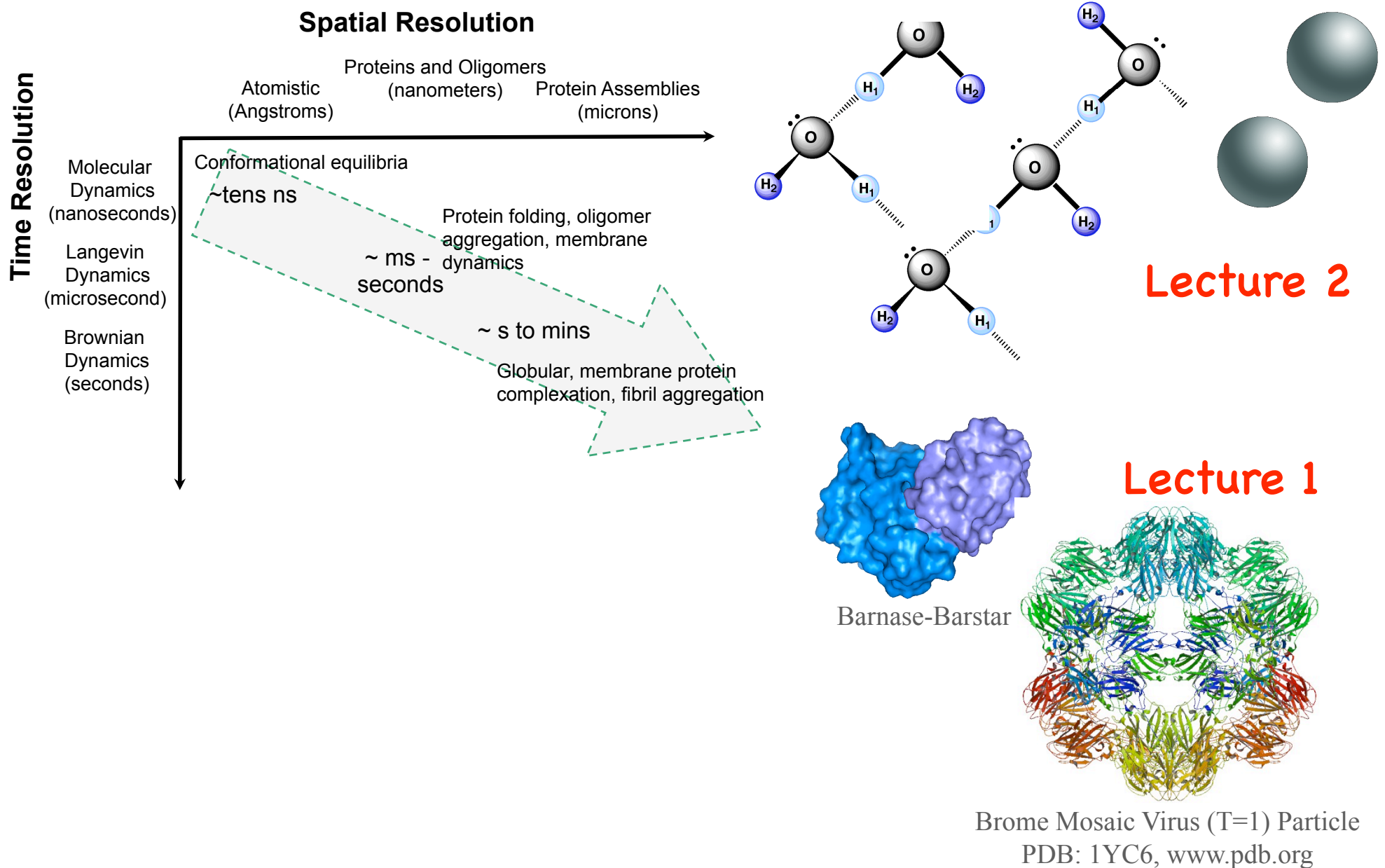
## Lecture 1



Brome Mosaic Virus (T=1) Particle  
PDB: 1YC6, [www.pdb.org](http://www.pdb.org)

## Lecture 2

# Coarse-Graining and MultiScale



# Theoretical Frameworks for Liquids

---

## The coarse-graining hierarchy for liquids

Quantum mechanics

Integrating out electrons to derive classical models

Eliminating N-body interactions and replace with effective 2-body interactions

Integrating out atoms or geometric degrees of freedom

## Purpose of these frameworks

To obtain a “realistic” model: a global view of the liquid by reproducing a wide range of reference data

To explore importance of underlying interactions: where does phenomena derive from?

# Representability Problems

---

Generalized proof that a unique set of interaction site potentials  $\{v_{\alpha\beta}\}$ , will produce a given set of site-site pair distribution functions  $\{g_{\alpha\beta}\}$  (structural coarse-graining)

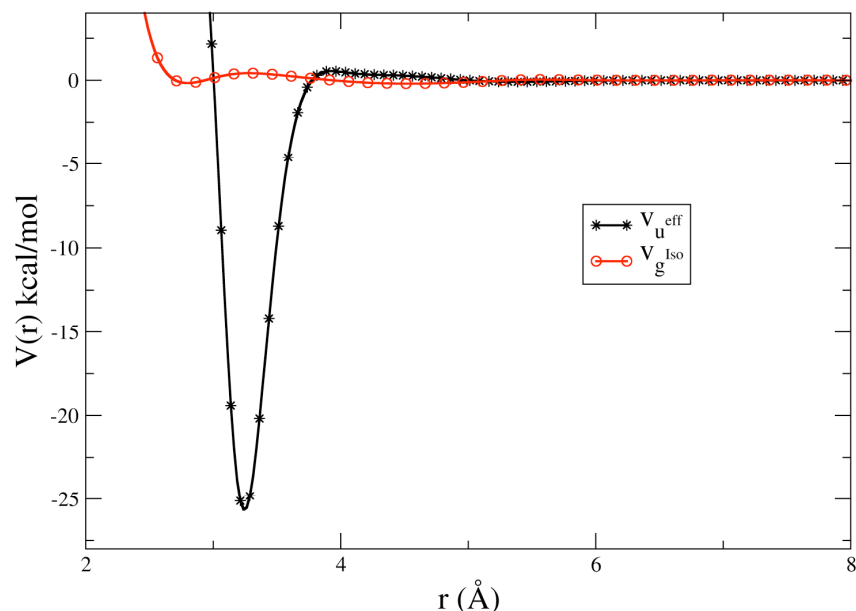
# Representability Problems

Generalized proof that a unique set of interaction site potentials  $\{v_{\alpha\beta}\}$ , will produce a given set of site-site pair distribution functions  $\{g_{\alpha\beta}\}$  (structural coarse-graining)

Can also coarse-grain through energy

$$U(N, V, T) = \frac{1}{2} \rho^2 \int d\mathbf{r}_1 d\mathbf{r}_2 g(r_{12}) v_U^{eff}(r_{12})$$

Gives very different results than coarse-graining through structure; but energy coarse-graining is not unique!



\*Johnson, THG, Louis (2007). *JCP* 126, 144509

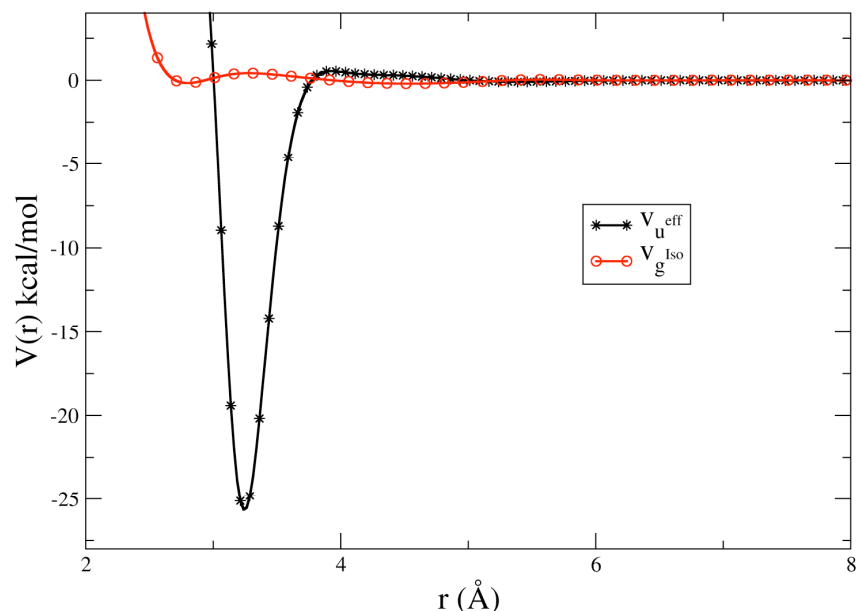
# Representability Problems

Generalized proof that a unique set of interaction site potentials  $\{v_{\alpha\beta}\}$ , will produce a given set of site-site pair distribution functions  $\{g_{\alpha\beta}\}$  (structural coarse-graining)

Can also coarse-grain through energy

$$U(N, V, T) = \frac{1}{2} \rho^2 \int d\mathbf{r}_1 d\mathbf{r}_2 g(r_{12}) v_U^{eff}(r_{12})$$

Gives very different results than coarse-graining through structure; but energy coarse-graining is not unique!



The uniqueness property of the coarse-grained structure route allow us to think about research problems for water!

\*Johnson, THG, Louis (2007). *JCP* 126, 144509

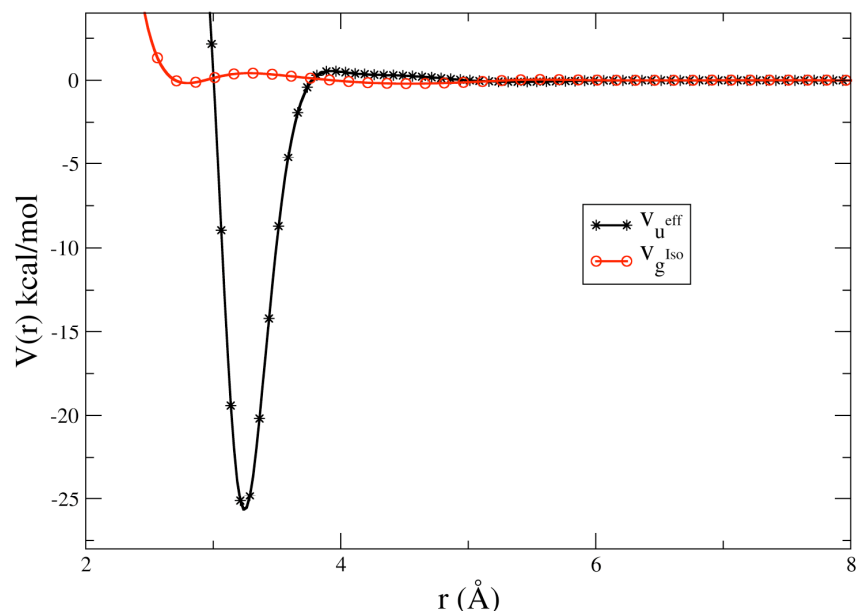
# Representability Problems

Generalized proof that a unique set of interaction site potentials  $\{v_{\alpha\beta}\}$ , will produce a given set of site-site pair distribution functions  $\{g_{\alpha\beta}\}$  (structural coarse-graining)

Can also coarse-grain through energy

$$U(N, V, T) = \frac{1}{2} \rho^2 \int d\mathbf{r}_1 d\mathbf{r}_2 g(r_{12}) v_U^{eff}(r_{12})$$

Gives very different results than coarse-graining through structure; but energy coarse-graining is not unique!

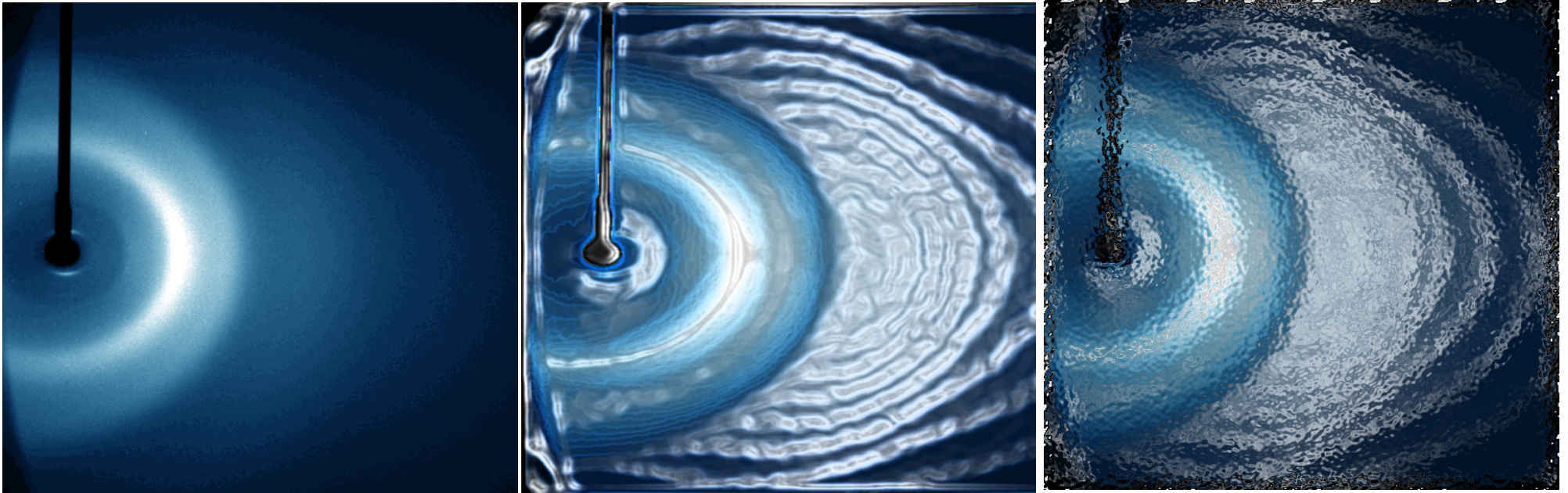


The uniqueness property of the coarse-grained structure route allow us to think about research problems for water!

\*Johnson, THG, Louis (2007). *JCP* 126, 144509

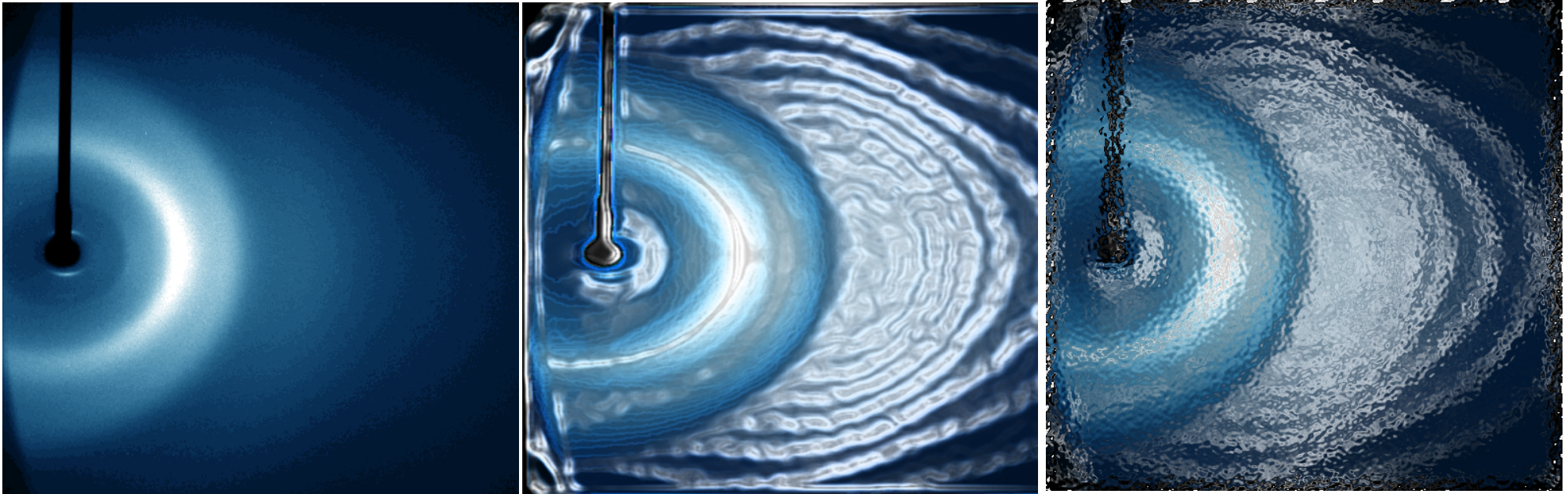


# Liquid Water Structure



Structure is our most tangible connection to understanding basic thermodynamic and dynamic properties of materials

# Liquid Water Structure



Structure is our most tangible connection to understanding basic thermodynamic and dynamic properties of materials

For bulk water and aqueous solvent

*Thermodynamic and possibly dynamic anomalies of bulk liquid*

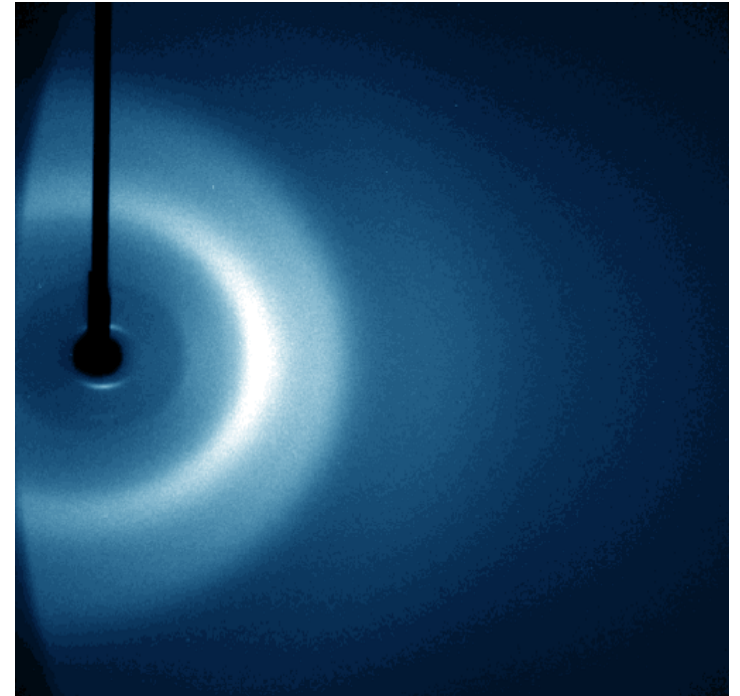
*Aqueous solvation: hydrophobic hydration, hydrogen-bonding*

*Theory, models and emerging simulation methodologies*

# Determining Liquid Water Structure

---

Water structure can be determined by x-ray (and neutron) scattering.



# Determining Liquid Water Structure

Water structure can be determined by x-ray (and neutron) scattering.

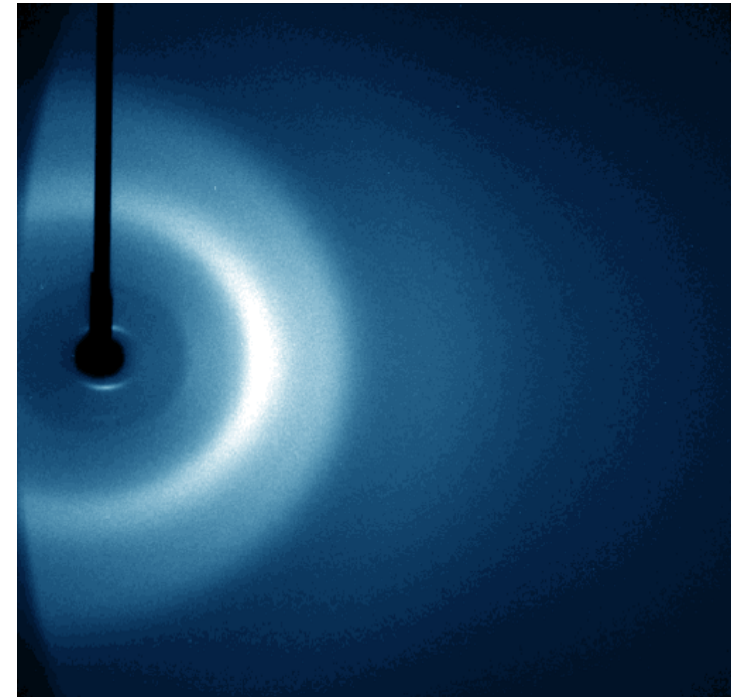
X-rays are scattered by sinusoidal components of electron density. The observable is the intensity which varies with momentum transfer  $Q$ .

$$Q = 4\pi \sin(\theta / 2) / \lambda$$

where  $\lambda$  is radiation wavelength and  $\theta$  is the scattering angle.

For each value of  $Q$  there is an (effective) Bragg spacing,  $d$ ,

$$d = \frac{\lambda}{2 \sin(\theta / 2)} = \frac{2\pi}{Q}$$



# Determining Liquid Water Structure

Water structure can be determined by x-ray (and neutron) scattering.

X-rays are scattered by sinusoidal components of electron density. The observable is the intensity which varies with momentum transfer  $Q$ .

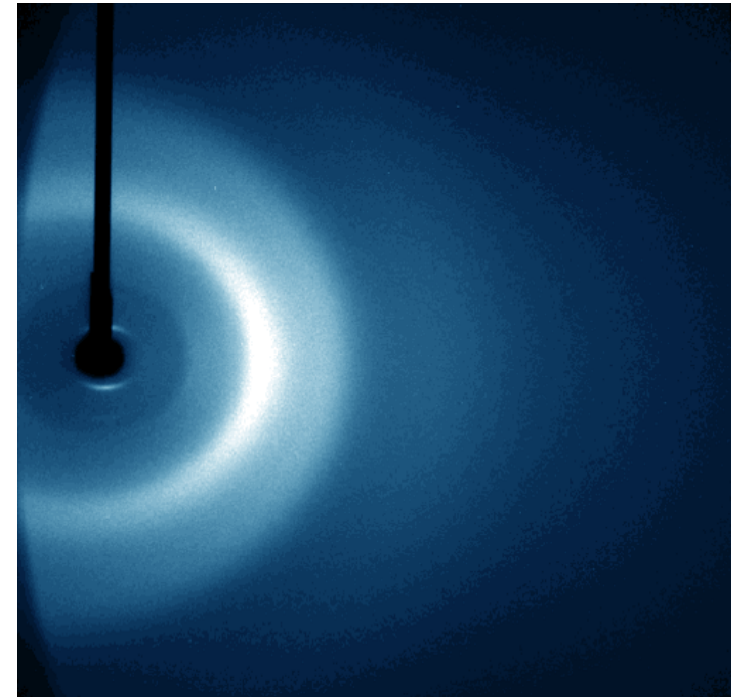
$$Q = 4\pi \sin(\theta / 2) / \lambda$$

where  $\lambda$  is radiation wavelength and  $\theta$  is the scattering angle.

For each value of  $Q$  there is an (effective) Bragg spacing,  $d$ ,

$$d = \frac{\lambda}{2 \sin(\theta / 2)} = \frac{2\pi}{Q}$$

In hexagonal ice,  $d \sim 0.39\text{nm}$  while in liquid water,  $d \sim 3.1\text{nm}$

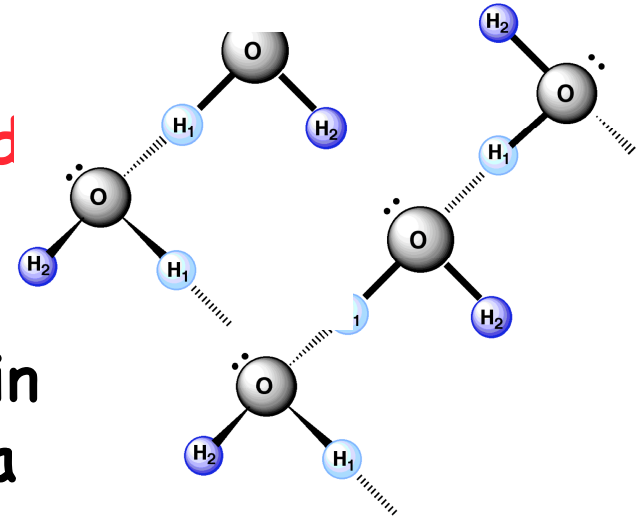


# Water is a Tetrahedral Liquid

---

Fundamental molecular unit of ice and liquid water structure is the hydrogen bond

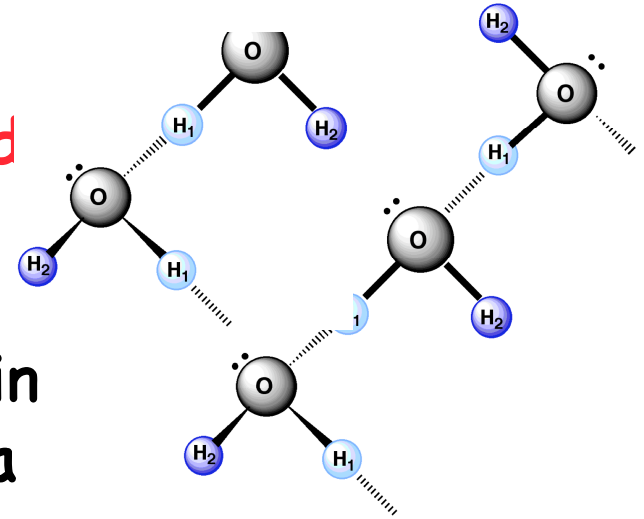
In hexagonal ice, a given water molecule is hydrogen-bonded to four water neighbors in a tetrahedral structure that gives rise to a crystal made up of hydrogen-bonded hexagonal rings (Bragg spacing  $3.9\text{\AA}$ ).



# Water is a Tetrahedral Liquid

Fundamental molecular unit of ice and liquid water structure is the hydrogen bond

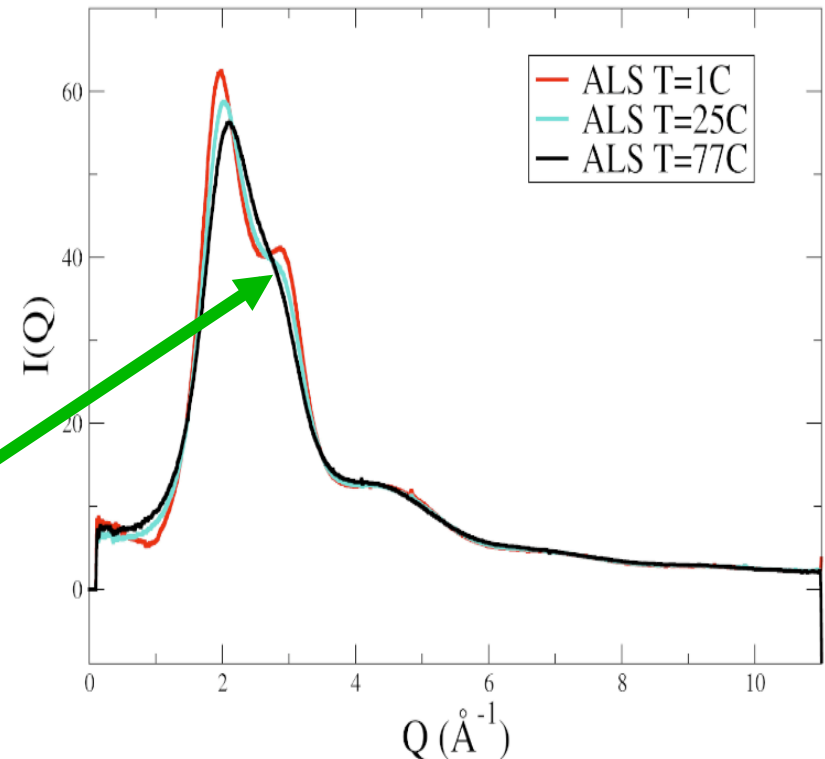
In hexagonal ice, a given water molecule is hydrogen-bonded to four water neighbors in a tetrahedral structure that gives rise to a crystal made up of hydrogen-bonded hexagonal rings (Bragg spacing  $3.9\text{\AA}$ ).



In liquid water, hydrogen-bonds distort under thermal fluctuations to give rise to broader distribution of water neighbor configurations, with decrease in effective Bragg spacing ( $3.1\text{\AA}$ ).

Details of hydrogen-bonding geometry in the first coordination shell are not directly available

# Tetrahedral Signatures of Bulk Liquid Water

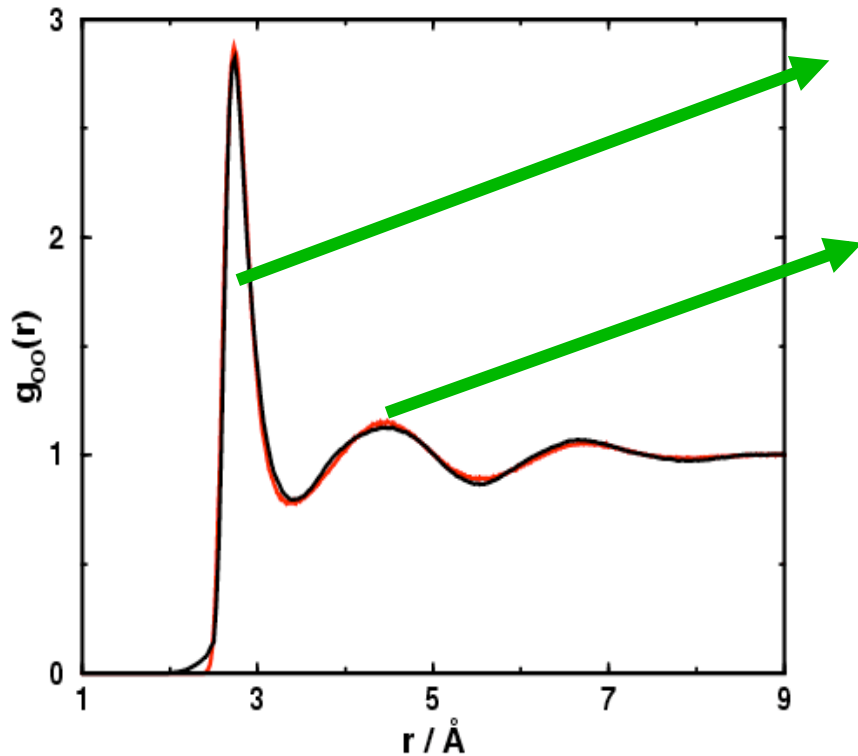


*Intensity shoulder at  $Q \sim 3.0\text{\AA}^{-1}$  (with  $d \sim 2.0\text{\AA}$ ) can be usefully viewed as an order parameter for tetrahedral structure since it sharpens at low  $T$*

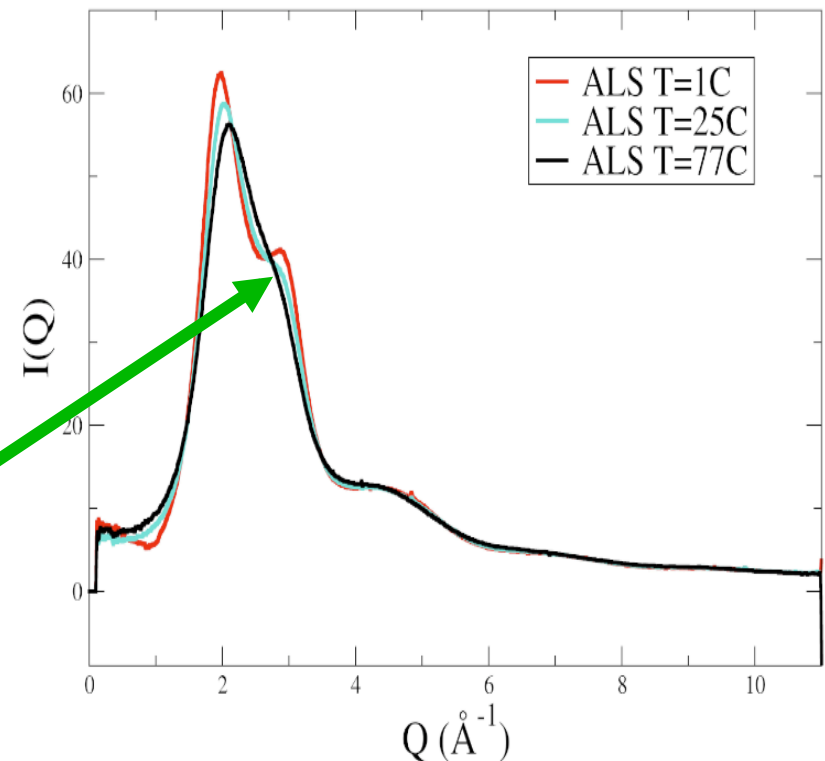


# Tetrahedral Signatures of Bulk Liquid

## Water



*Integration under first peak of  $g_{OO}$  gives coordination number of  $\sim 4.7$  and strong peak at  $r \sim 4.5 \text{\AA}$  suggests that liquid water retains significant tetrahedral structure*



*Intensity shoulder at  $Q \sim 3.0 \text{\AA}^{-1}$  (with  $d \sim 2.0 \text{\AA}$ ) can be usefully viewed as an order parameter for tetrahedral structure since it sharpens at low  $T$*

Head-Gordon and Johnson (2006). *PNAS* 103, 7973-7977.

# Calculating Intensity Classical/Quantum Model

---

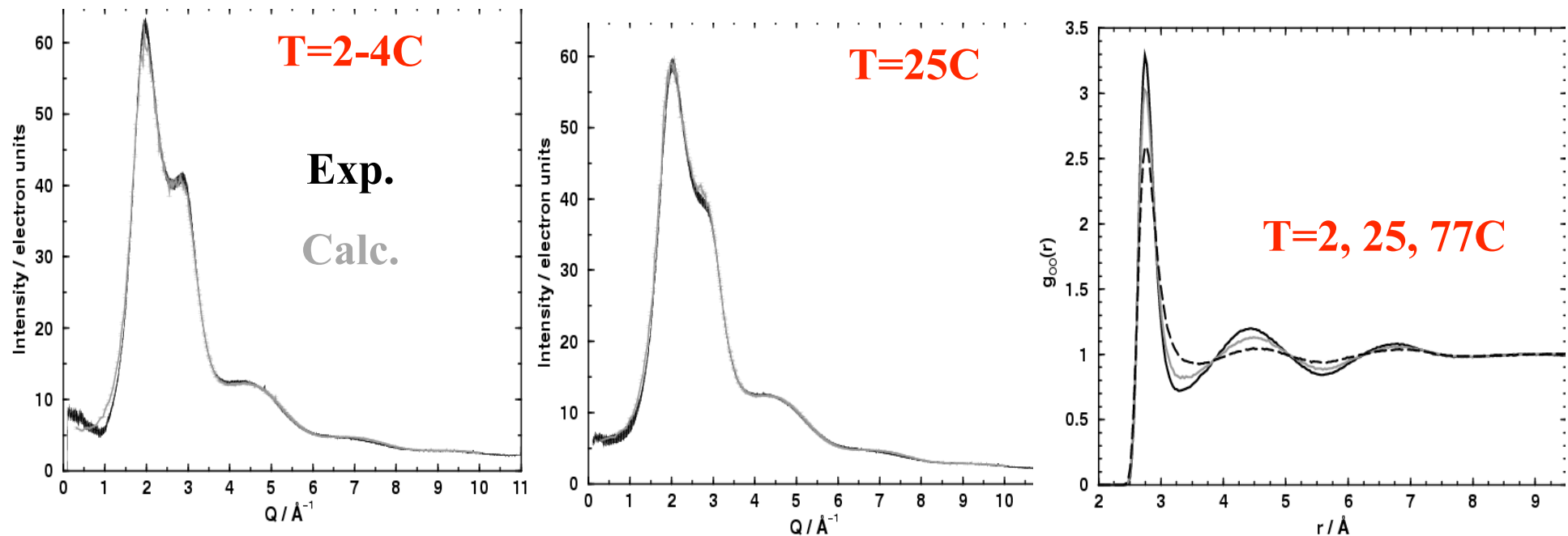
*Intensity determined from DFT densities and integration is from classical water model simulation*

$$I(Q) = \langle |F(Q)|^2 \rangle \quad \rightarrow \quad F(Q) = \int \rho(r) \exp(iQ \cdot r)$$

# Classical/Quantum Model

Intensity determined from DFT densities and integration is from classical water model simulation

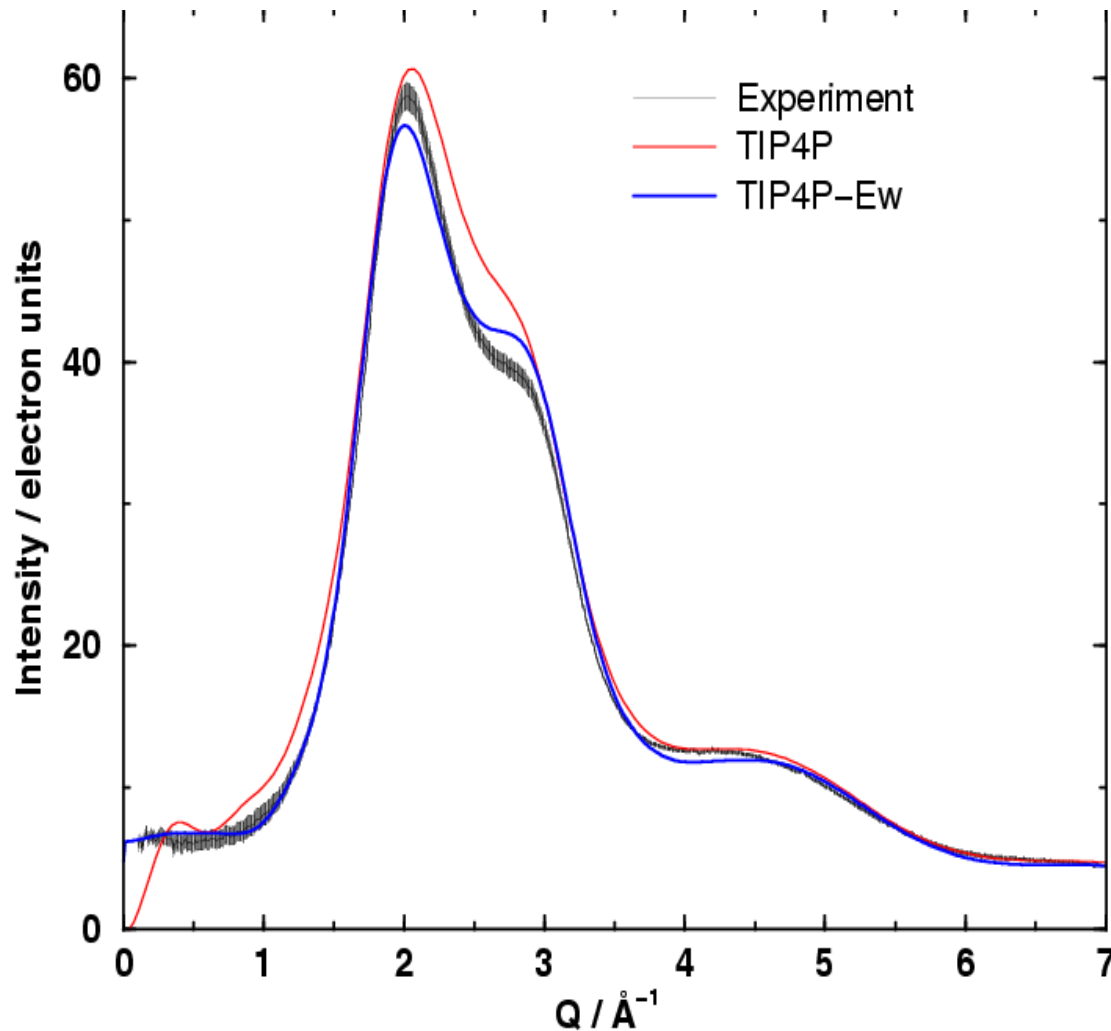
$$I(Q) = \langle |F(Q)|^2 \rangle \rightarrow F(Q) = \int \rho(r) \exp(iQ \cdot r)$$



Configurations based on classical polarizable water model  
TIP4P-Pol2, Chen & Siepmann

Hura, Russo, Glaeser, Krack, Parrinello & Head-Gordon (2003). *PCCP* 113, 9149-9161.

# Non-Polarizable Water Model with Ewald: TIP4P-EW

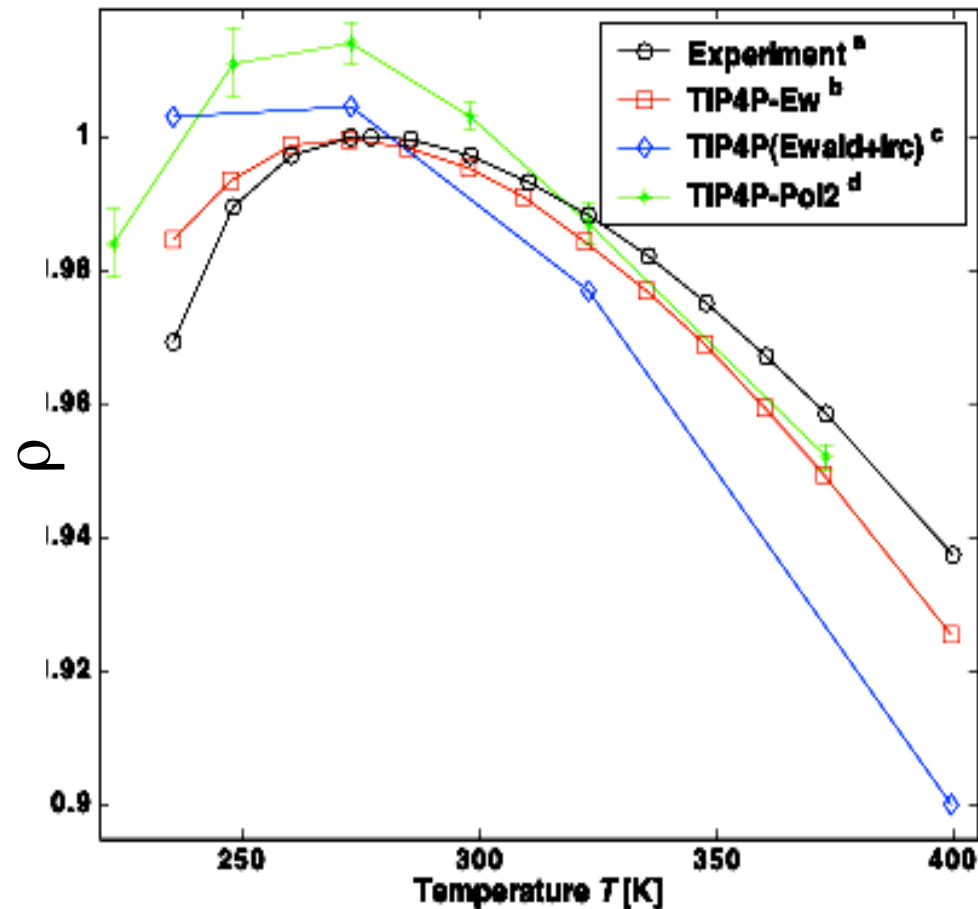


A re-parameterization of popular TIP4P water model for use with Ewald techniques provides an overall improvement in water structure

Horn, Swope, Pitara, Madura, Dick, Hura & Head-Gordon (2004). *JCP*.

# TIP4P-EW: a new accurate water model over a wide temperature range

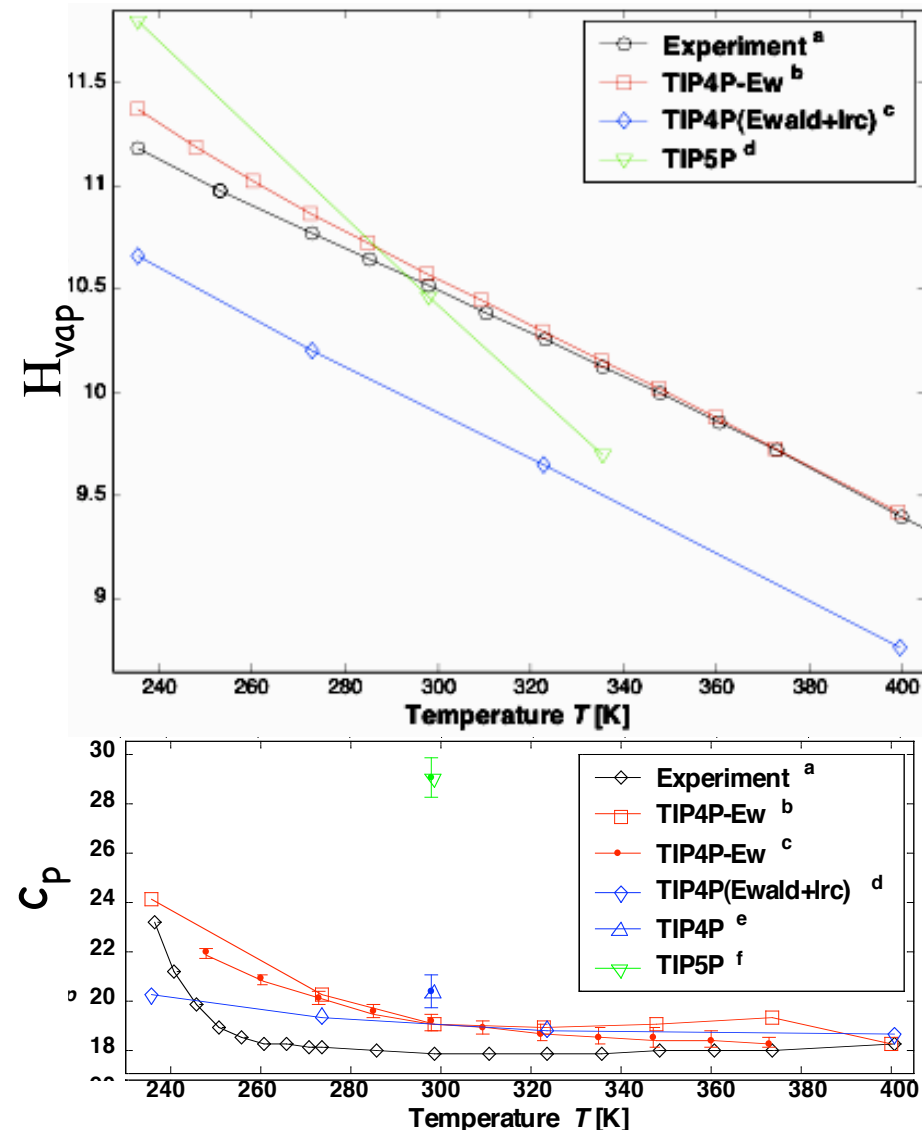
Reproduces experimental bulk-densities from -37.5 to 127C at 1atm with an absolute average error of less than 1%.



Horn, Swope, Pitara, Madura, Dick, Hura & Head-Gordon (2004). *JCP*.

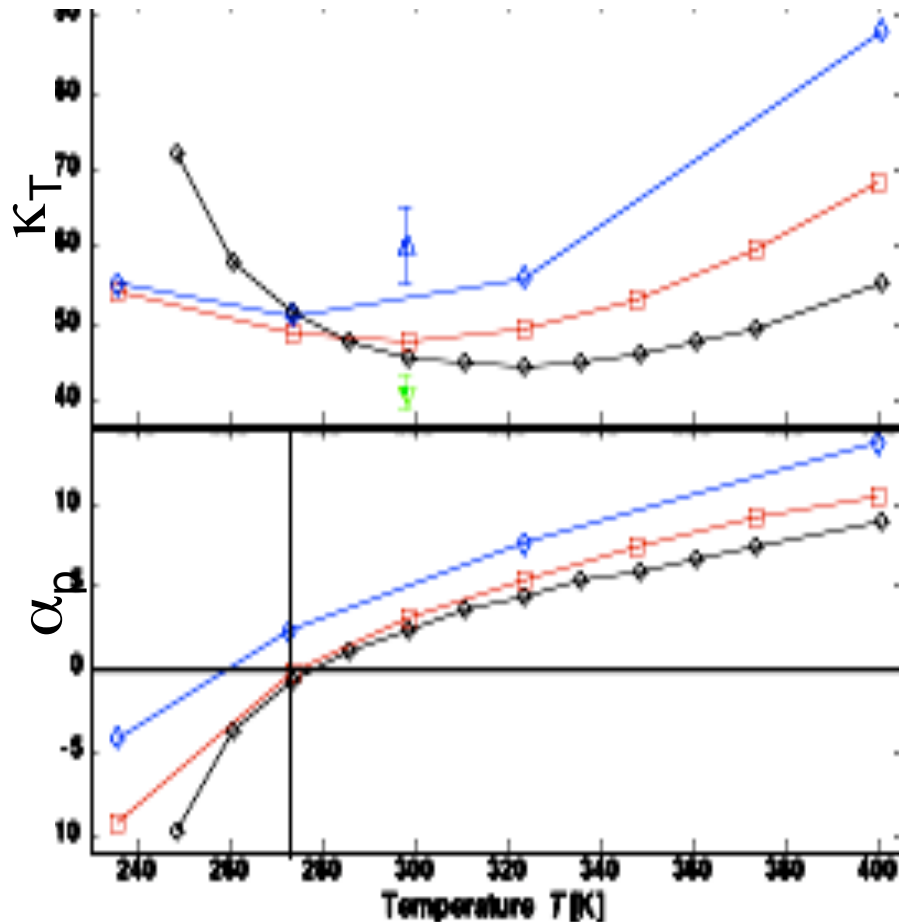
# TIP4P-EW: Thermodynamic Properties

TIP4P-Ew shows excellent agreement with enthalpy of vaporization, although the slope of the TIP4P-Ew curve is marginally steeper than experimental curve, which manifests itself in heat capacities  $c_p(T)$  that are slightly too high.



Horn, Swope, Pitara, Madura, Dick, Hura & Head-Gordon (2004). *JCP*.

# TIP4P-EW: Fluctuation Properties



Isothermal compressibility  $\kappa_T(T)$  is within  $\sim 8\%$  of experiment

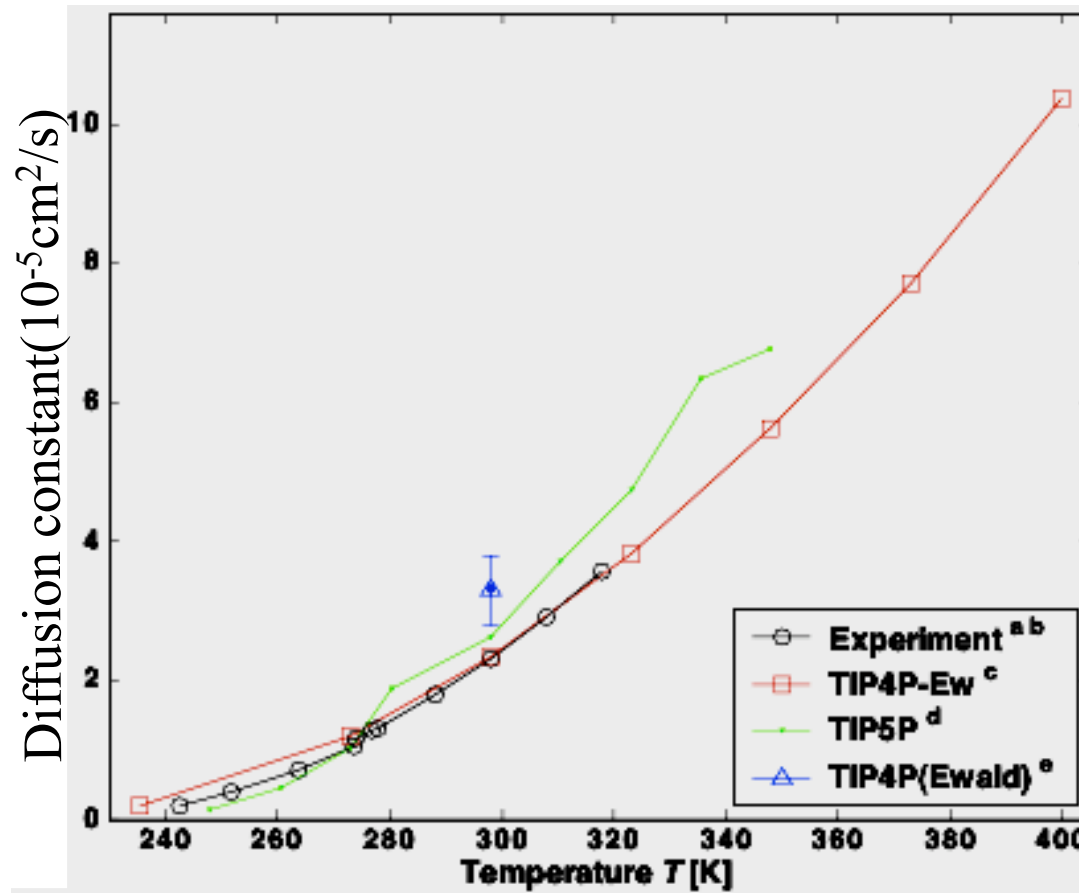
Thermal expansion coefficient  $\alpha_p(T)$  is within  $10^{-4}\text{K}^{-1}$  of experiment, between 273K and 310K.

The thermal expansion coefficient is zero at TMD  $\sim 274\text{K}$ .

Horn, Swope, Pitner, Madura, Dick, Hura & Head-Gordon (2004). *JCP*.

# TIP4P-EW: Dynamical Properties

TIP4P-Ew has excellent transport properties



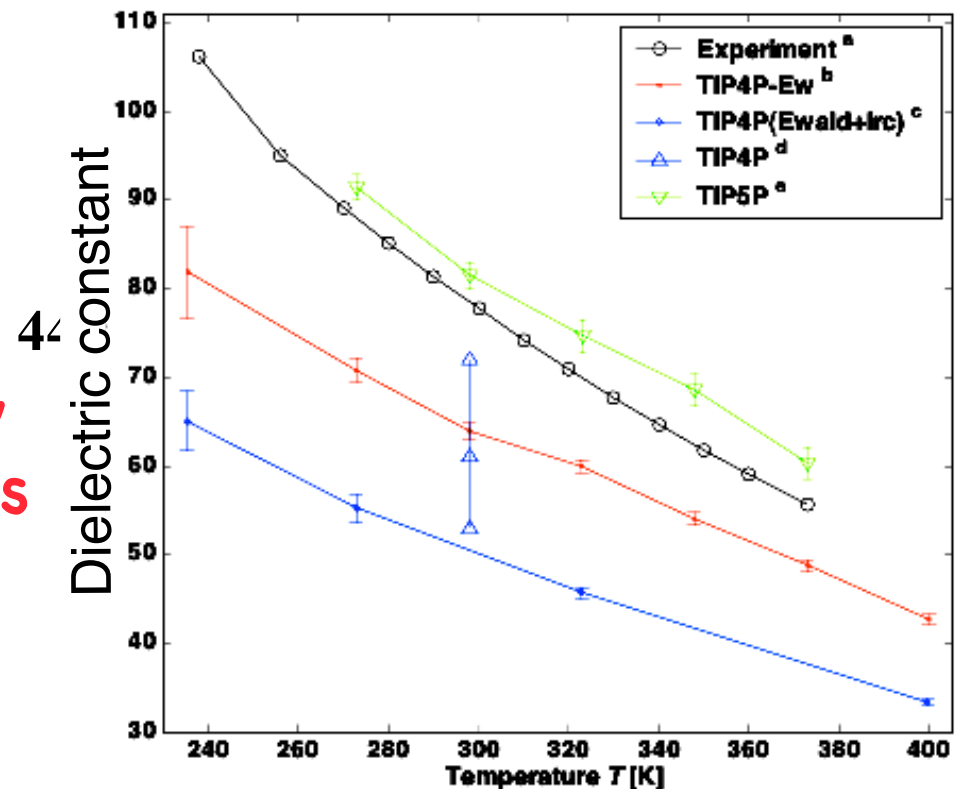
Horn, Swope, Pitner, Madura, Dick, Hura & Head-Gordon (2004). *JCP*.



# TIP4P-EW: Dielectric Properties

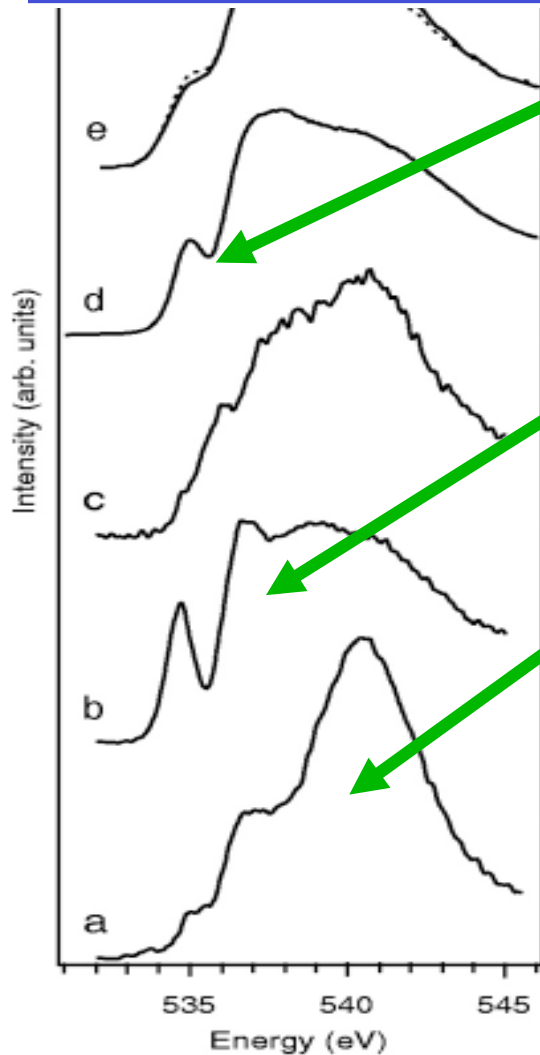
The overall agreement of TIP4P-Ew with experiment for static dielectric constant is not great (~15% error), but it halves the error for TIP4P in its original parameterization.

The static dielectric constant may be a water property that requires explicit polarization, inclusion of molecular flexibility, or use of something other than conducting boundary conditions.



Horn, Swope, Pitara, Madura, Dick, Hura & Head-Gordon (2004). *JCP*.

# XAS Experiments on Liquid Water



(d) Liquid water at ambient conditions

(b) Ice Ih surface (~50% broken h-bonds)

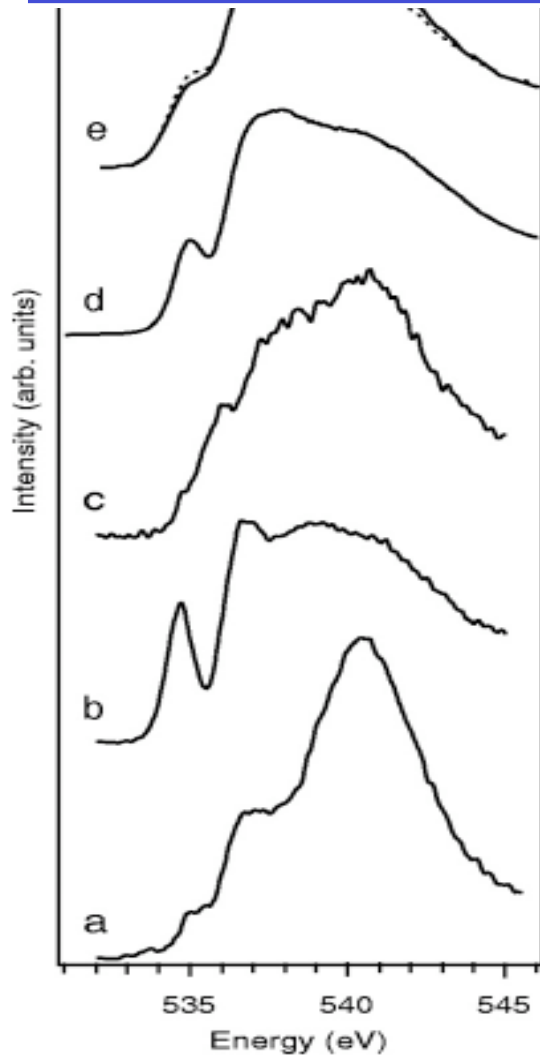
(a) Bulk ice Ih (tetrahedral, 4 h-bonds)

Pre-edge peak in x-ray absorption spectroscopy (EXAFS) of liquid water resembles the ice surface, suggesting significant reduction in hydrogen bonds with respect to bulk ice

Wernet et al. *Science* 2004

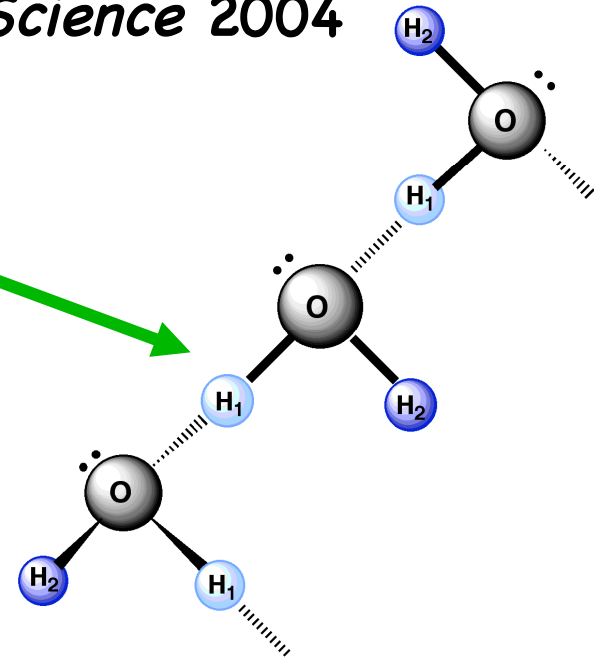
Lecture 2

# XAS Interpretations of Liquid Water



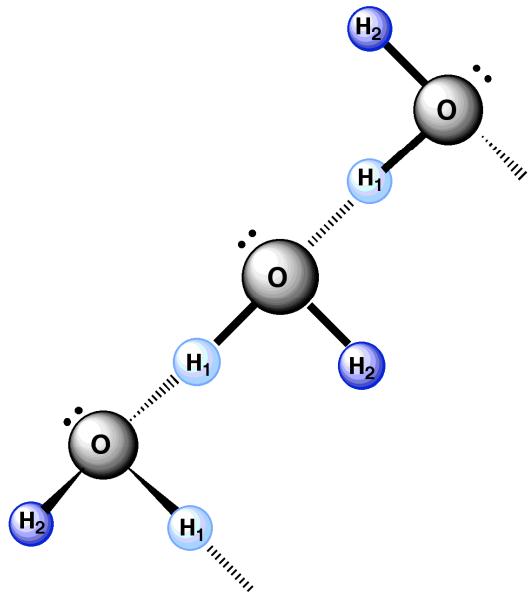
“The present result that water, on the probed subfemtosecond time scale, consists mainly of structures with two strong H-bonds, one donating and one accepting, implies that most molecules are arranged in strongly H-bonded chains or rings embedded in a disordered cluster network connected mainly by weak H-bonds.”

Wernet et al. *Science* 2004



# XAS Interpretations of Liquid Water

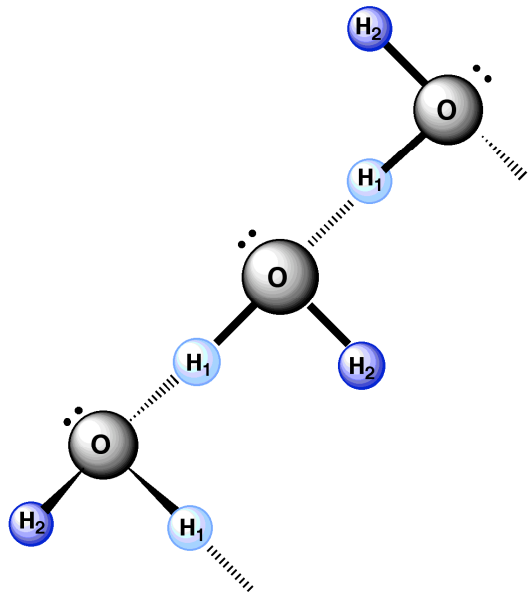
---



"....the cutting-edge SRL at Stanford University seems to have little in common with new-age drinks or alternative medicine. But that was before plain old water- the most abundant substance on Earth, the basis of life, a compound whose structure was probed during Queen Victoria's reign- turned out to have fooled a long line of scientists.

"It's such a basic question, the structure of water," says chemical physicist Anders Nilsson of Stanford. "It's amazing we don't really understand it."

# XAS Interpretations of Liquid Water



"...the cutting-edge SRL at Stanford University seems to have little in common with new-age drinks or alternative medicine. But that was before plain old water- the most abundant substance on Earth, the basis of life, a compound whose structure was probed during Queen Victoria's reign- turned out to have fooled a long line of scientists.

"It's such a basic question, the structure of water," says chemical physicist Anders Nilsson of Stanford. "It's amazing we don't really understand it."

The notion that water molecules form pyramids actually had little empirical support, Dr. Nilsson says: "Experimental findings have been so sparse that theoretical work has dominated the field," and the theory is so inexact "that you can get almost any result you want just by tweaking" a few numbers.

# Water with Asymmetric Charge Density

---

The ESPR method was used to develop a 3D model of liquid water that conforms to both neutron and x-ray diffraction data

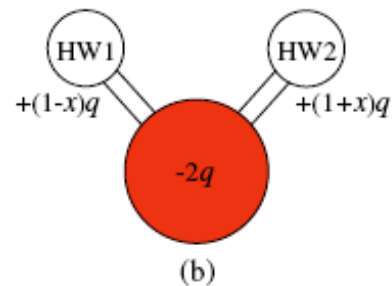
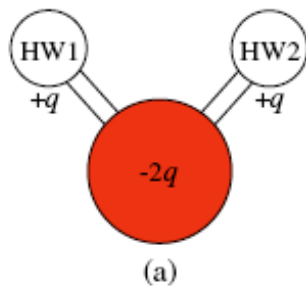
$$V_{\alpha\beta}(r) = V_{\alpha\beta}^{ref}(r) + k_b T \ln \left[ g_{\alpha\beta}^{Calc}(r) / g_{\alpha\beta}^{Expt}(r) \right]$$

# Water with Asymmetric Charge Density

The ESPR method was used to develop a 3D model of liquid water that conforms to both neutron and x-ray diffraction data

$$V_{\alpha\beta}(\mathbf{r}) = V_{\alpha\beta}^{ref}(\mathbf{r}) + k_b T \ln \left[ g_{\alpha\beta}^{Calc}(\mathbf{r}) / g_{\alpha\beta}^{Expt}(\mathbf{r}) \right]$$

The reference potential is based on asymmetry in the hydrogen electron density as proposed by Wernet et al



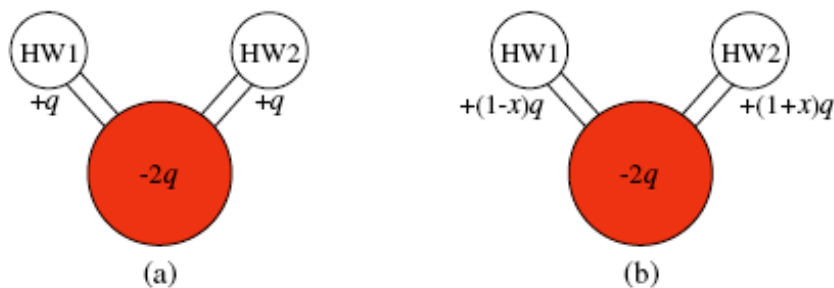
$$qH_1 = 0.6e, \quad qH_2 = 0.0e, \quad qO = -0.6e$$

# Water with Asymmetric Charge Density

The ESPR method was used to develop a 3D model of liquid water that conforms to both neutron and x-ray diffraction data

$$V_{\alpha\beta}(r) = V_{\alpha\beta}^{ref}(r) + k_b T \ln \left[ g_{\alpha\beta}^{Calc}(r) / g_{\alpha\beta}^{Expt}(r) \right]$$

The reference potential is based on asymmetry in the hydrogen electron density as proposed by Wernet et al



$$qH_1 = 0.6e, \quad qH_2 = 0.0e, \quad qO = -0.6e$$

Based on definition of intact hydrogen-bond,

$$R_{OO}(\theta) = 3.3 - 0.00044\theta^2 \quad (\text{Wernet et al, 2004})$$

SoperAsym model gives  $\langle 2 \text{ h-bonds} \rangle$



# Model with Symmetric Charge Density

---

This is to be contrasted with a non-polarizable TIP4P-EW model that assumes a symmetric charge density

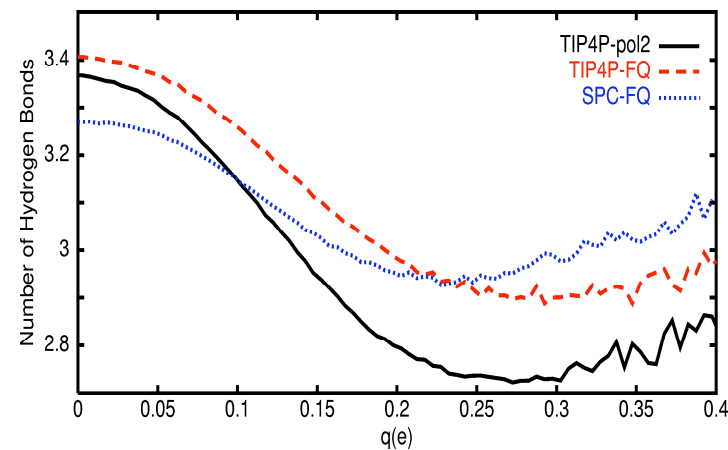
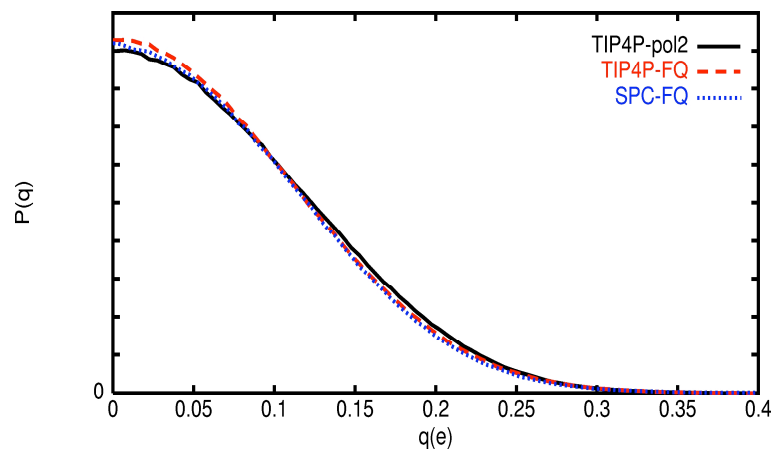
$$q_{H_1}=0.52422e \text{ and } q_{H_2}=0.52422e \text{ and } q_O=-1.04844e$$

# Model with Symmetric Charge Density

This is to be contrasted with a non-polarizable TIP4P-EW model that assumes a symmetric charge density

$$q_{H_1}=0.52422e \text{ and } q_{H_2}=0.52422e \text{ and } q_O=-1.04844e$$

Or a polarizable model that assumes an instantaneous charge asymmetry depending on local environment

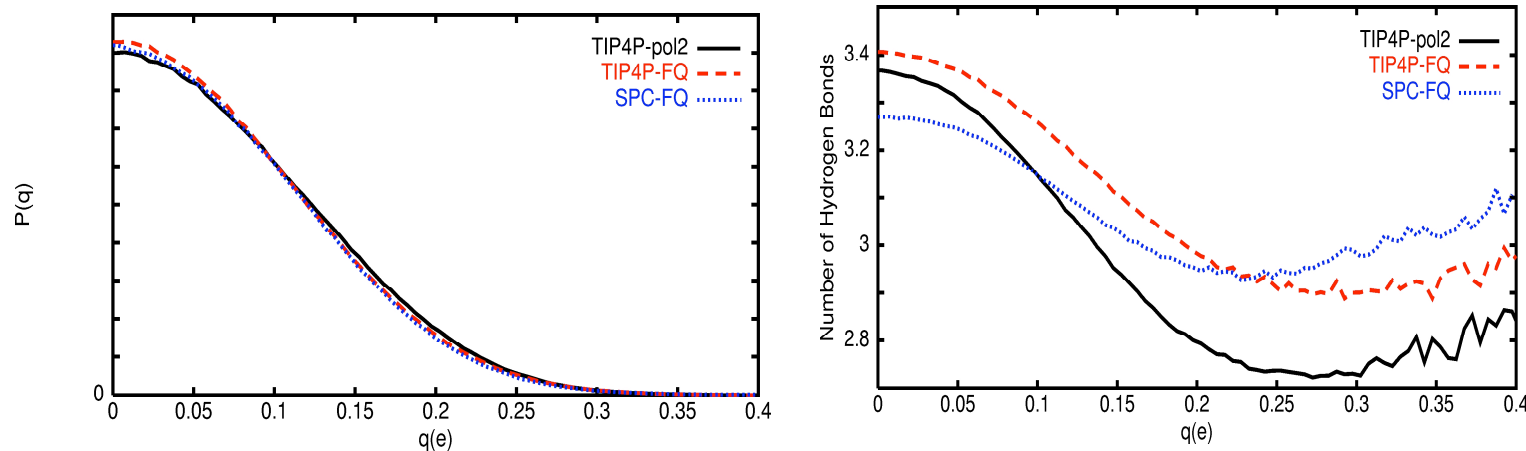


# Model with Symmetric Charge Density

This is to be contrasted with a non-polarizable TIP4P-EW model that assumes a symmetric charge density

$$q_{H_1}=0.52422e \text{ and } q_{H_2}=0.52422e \text{ and } q_O=-1.04844e$$

Or a polarizable model that assumes an instantaneous charge asymmetry depending on local environment



Based on definition of intact hydrogen-bond,

$$R_{OO}(\theta) = 3.3 - 0.00044\theta^2 \text{ (Wernet et al, 2004)}$$

<3-4 h-bonds>

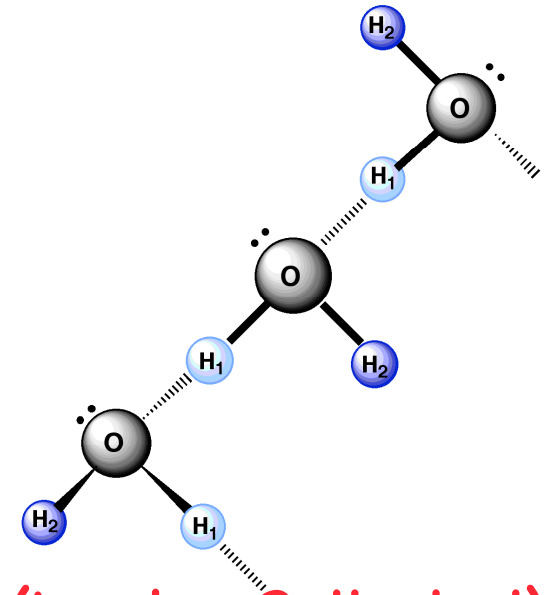
# Water Models that Exhibit Chain Networks

## Soper asymmetric model:

- SPC/E geometry
- hydrogen charge asymmetry
- ~2.5 h-bonds/water on average
- Supercritical (isobar 10000atm)
- dipole moment of 3.03 Debye
- first peak of g<sub>OO</sub>
- ~10kcal/molecule binding energy

## TIP4PEW Asymmetric model:

- TIP4P-EW geometry
- hydrogen charge asymmetry
- ~2.2 h-bonds/water on average
- Density is correct
- dipole moment of 2.3 Debye
- First peak of g<sub>OO</sub>
- ~11kcal/mole binding energy



## B60 model (Lynden-Bell et al):

- HOH angle=60°, r<sub>OH</sub>=0.6667Å
- hydrogen charge symmetry
- ~2.3 h-bonds/water on average
- Density correct
- dipole moment of 2.3 Debye
- first peak of g<sub>OO</sub>
- ~9kcal/molecule binding energy

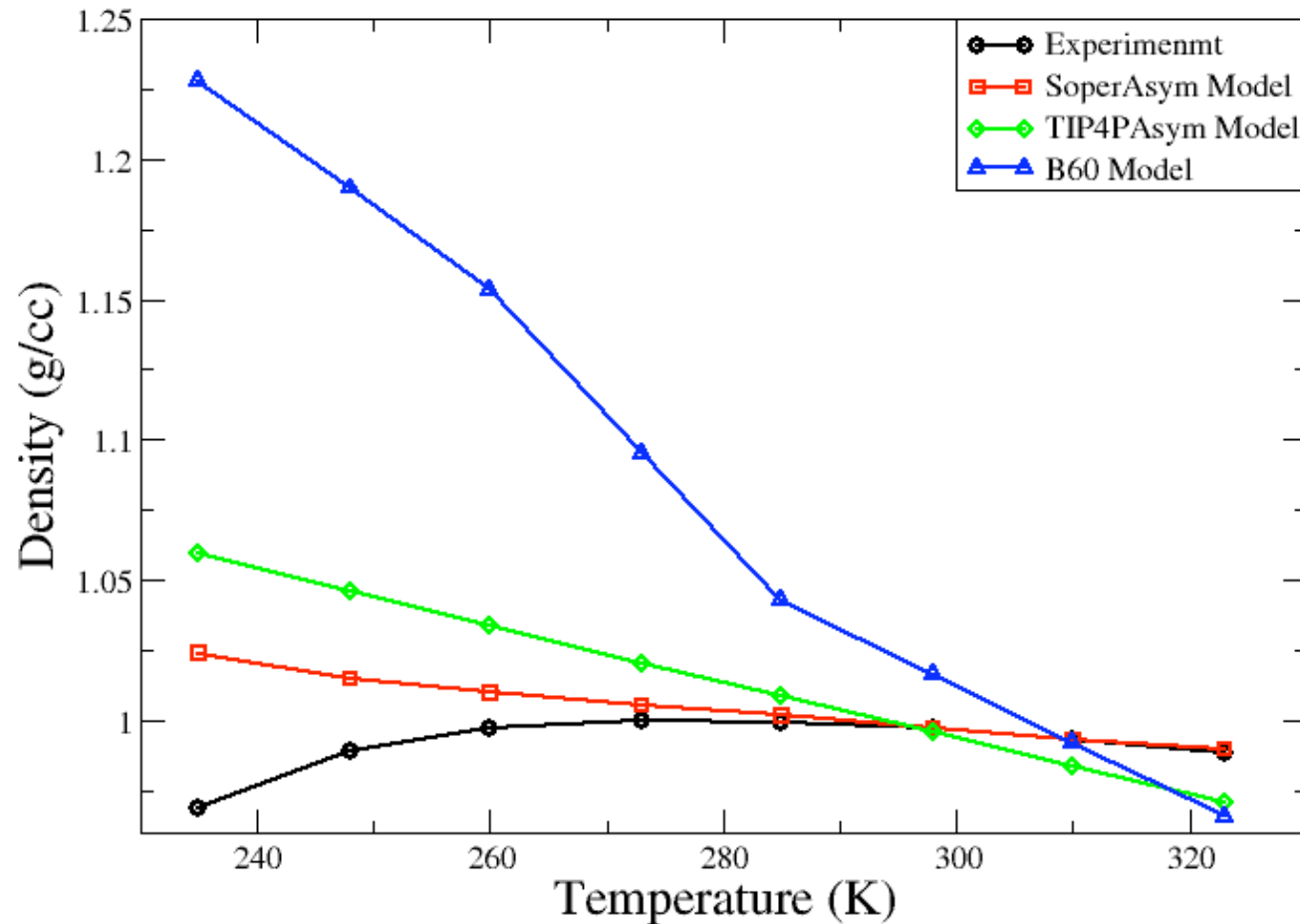
Head-Gordon & Rick (2007). "Hot Topic" PCCP

# Density as a Function of Temperature

Water's most famous anomaly is the TMD at 277K

All models show increasing densities w/ decreasing temperature

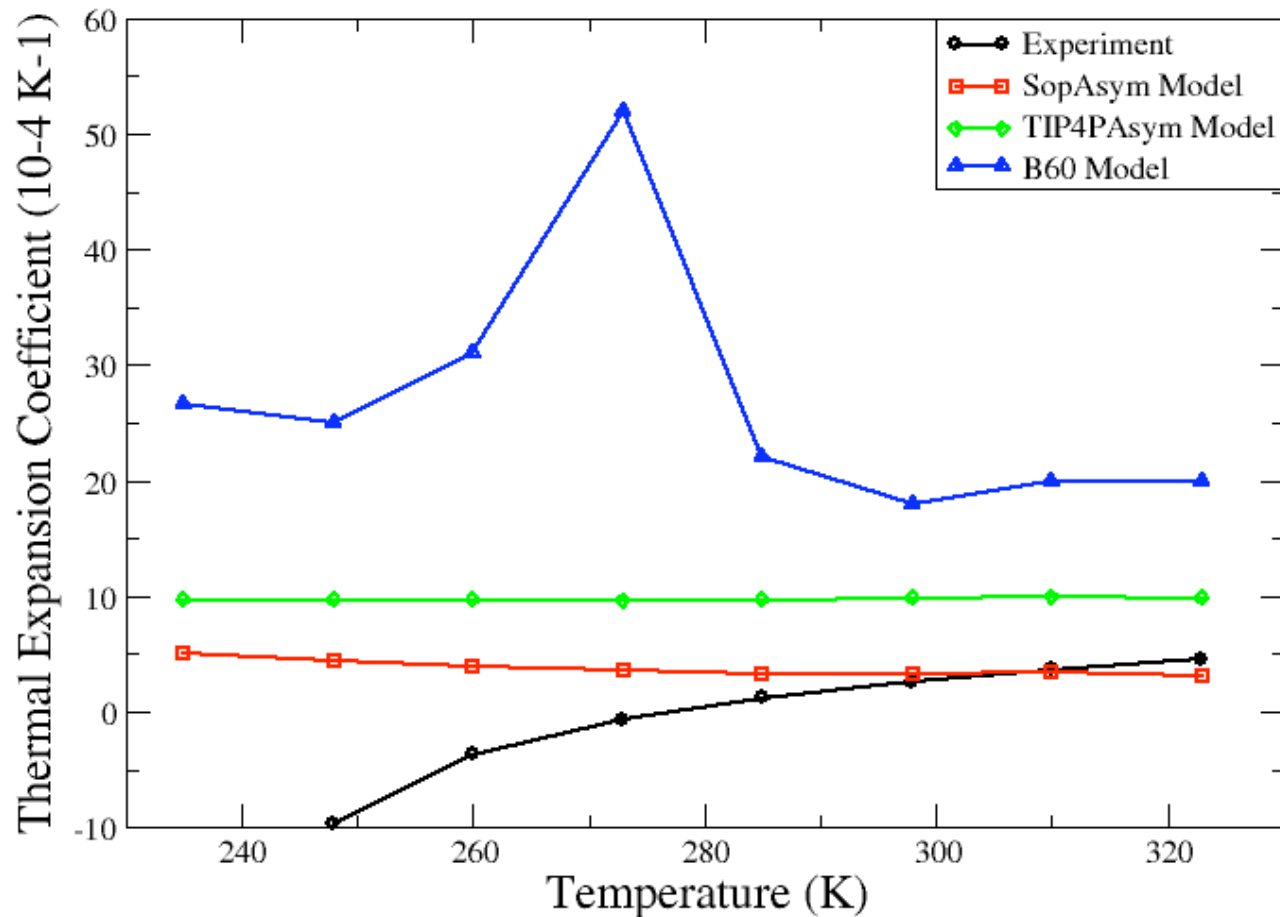
No TMD in sight!



Head-Gordon & Rick (2007). "Hot Topic" PCCP

# Thermal Expansion Coefficient

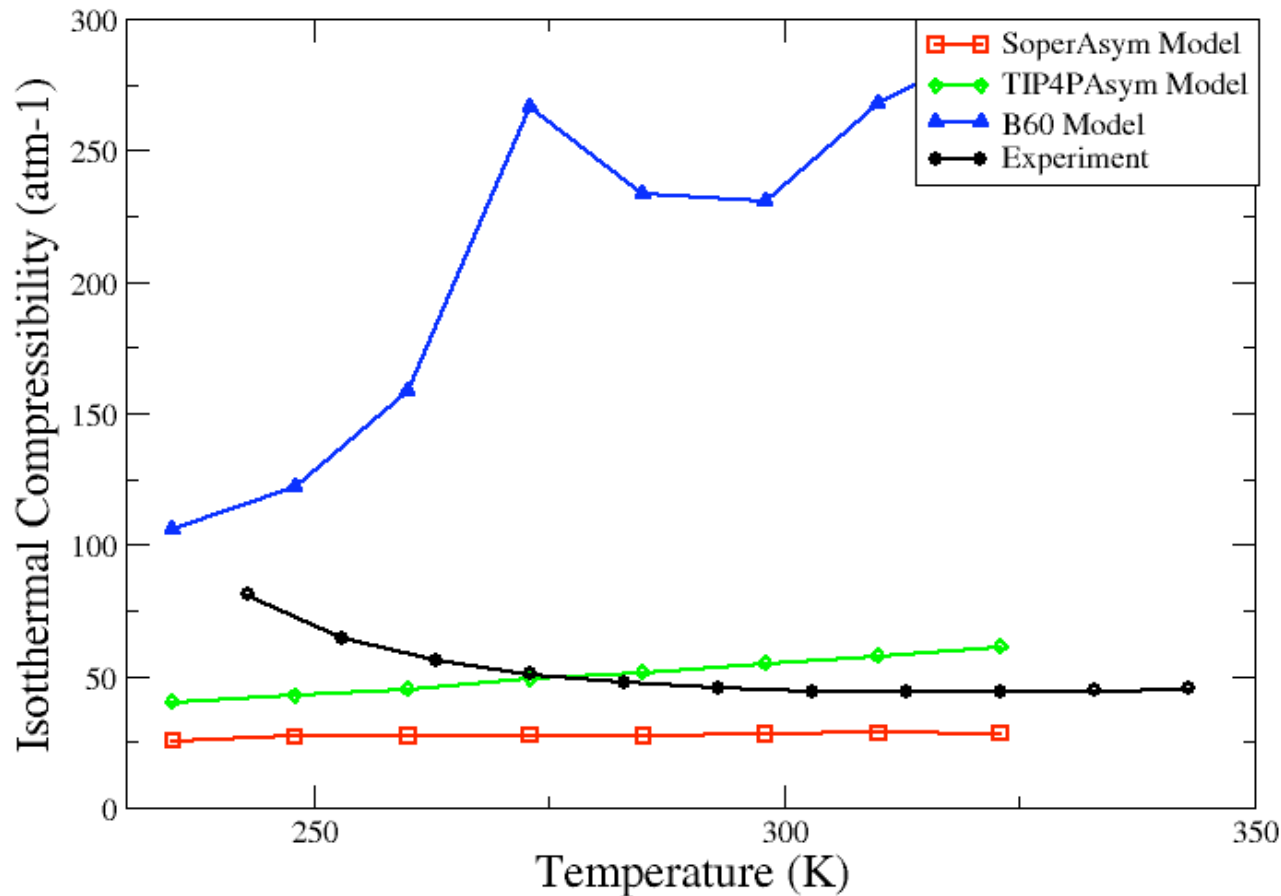
No TMD in sight and hence no negative thermal expansion coefficient at low temperatures (normal liquids)



Head-Gordon & Rick (2007). "Hot Topic" PCCP

# Isothermal Compressibility

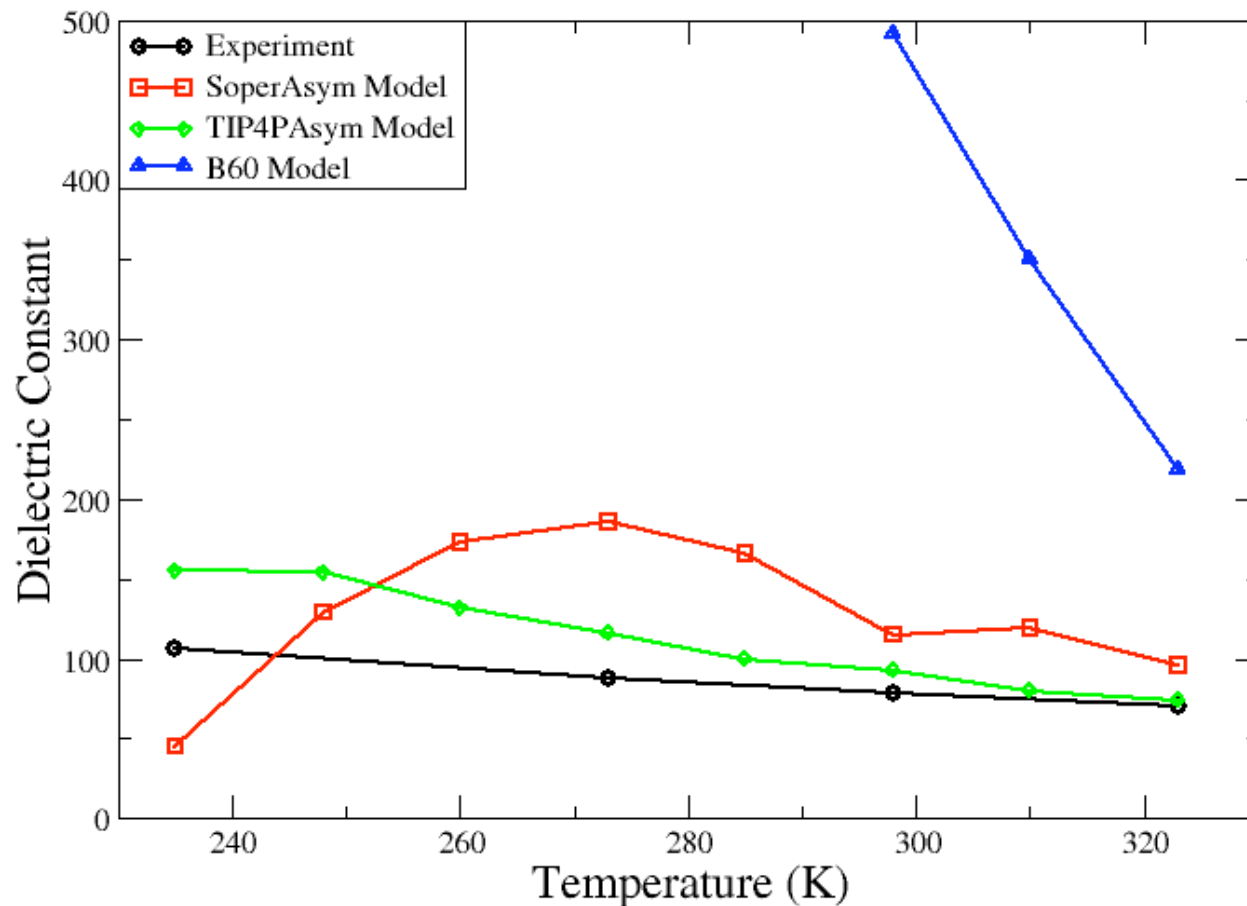
Anomalous decrease in isothermal compressibility as temperature is lowered is not reproduced by chain networks— all behave as normal fluids



Head-Gordon & Rick (2007). "Hot Topic" PCCP

# Dielectric Constant with Temperature

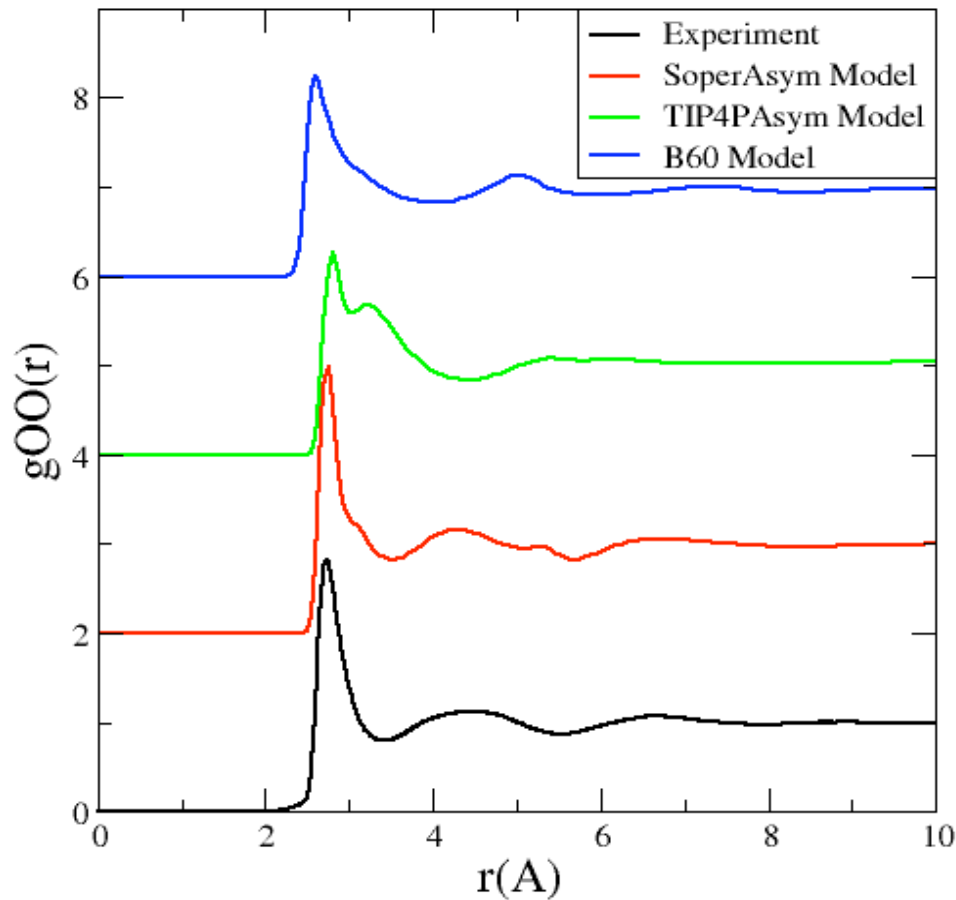
Greatly exaggerated with respect to water and more similar to other chain network fluids such as HF



Head-Gordon & Rick (2007). "Hot Topic" PCCP



# All Chain Network Models Show Anti-tetrahedral Structure!



In large measure,  
hydrogen-bonded chain  
networks behave as  
normal fluids

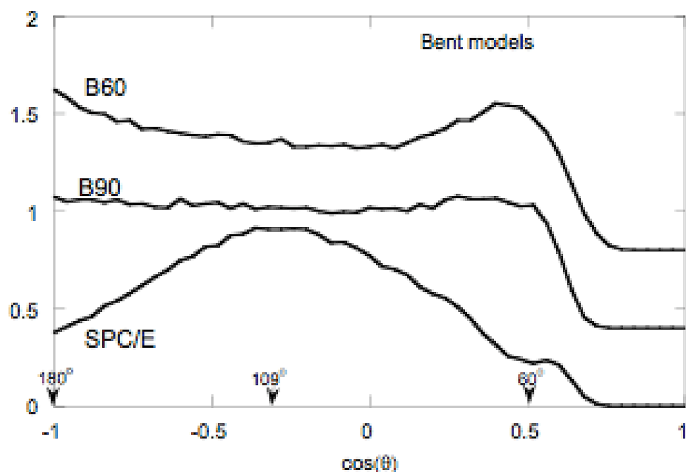
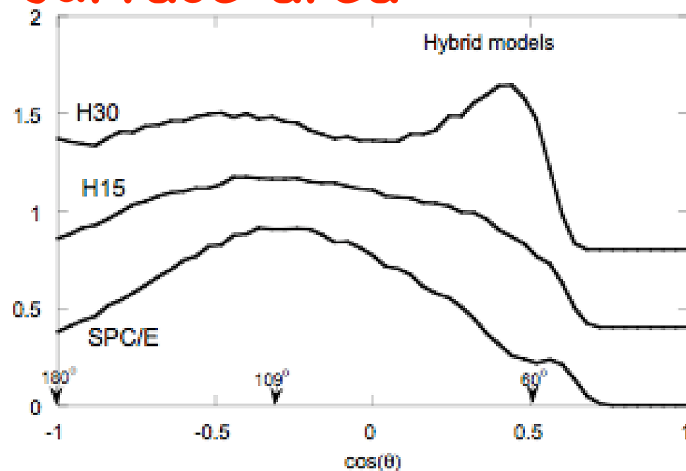
Tetrahedral order is our  
best "correlator" with  
water's thermodynamic  
properties

Head-Gordon & Rick (2007). "Hot Topic" PCCP

# Hydrophobicity at Different Lengthscales

At small lengthscales (comparable to a water diameter), hydrophobicity is controlled by volume voids in neat liquid

At large lengthscales, hydrophobicity is controlled by solute surface area



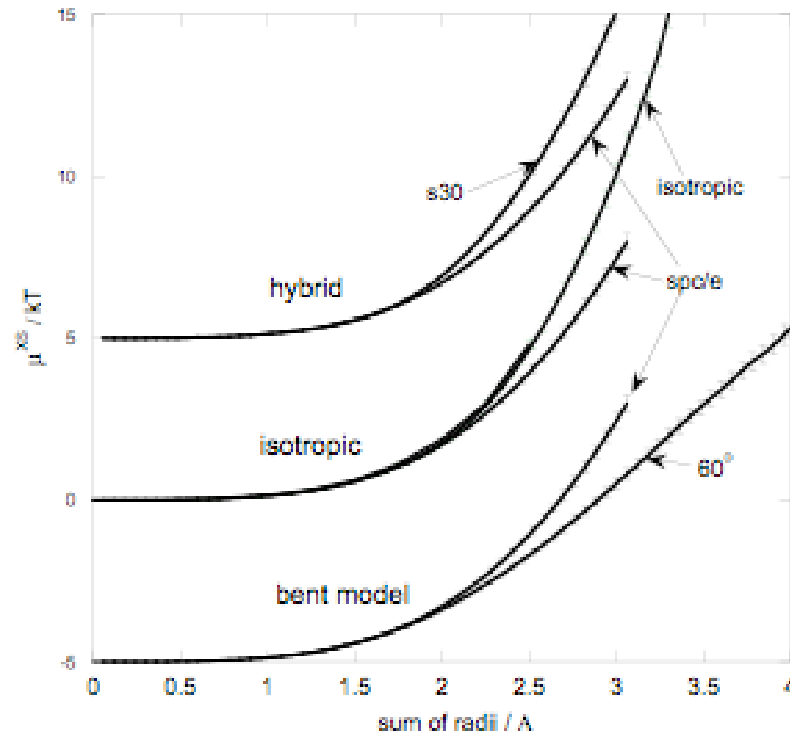
Hybrid Models (H15, H30) are blends of LJ and SPC/E water potentials. They reduce the h-bond interaction strength

Bent models (B60, B90) reduce the HOH angle of water to change tetrahedral network to linear networks

Lynden-Bell & Head-Gordon (2007). *Mol Phys* 104, 3593

# Hydrophobicity at Small Lengthscales

## Widom insertion of hard spheres



Nature could have devised more solvophobic liquids than water!

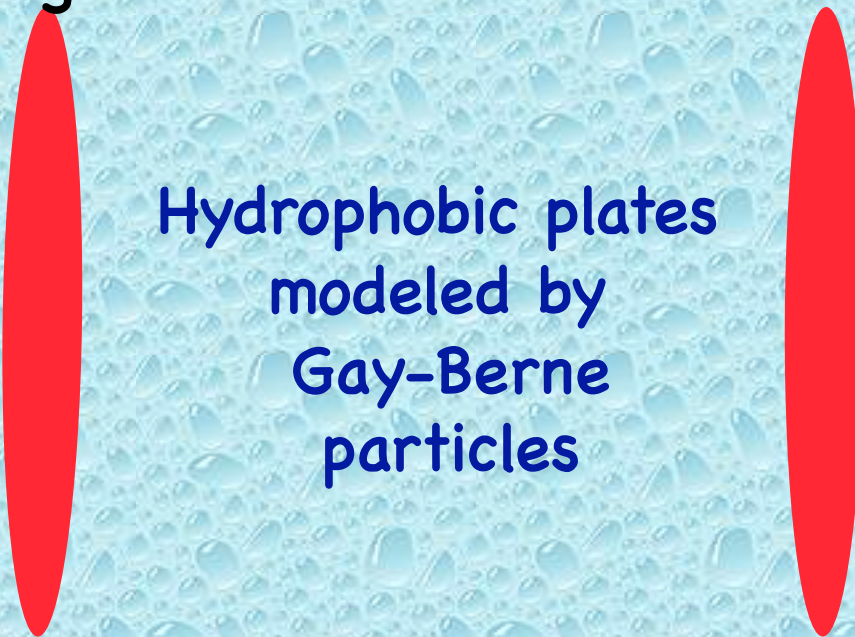
Lynden-Bell & Head-Gordon (2007). *Mol Phys* 104, 3593

Lecture 2

# Hydrophobicity at Large Lengthscales

---

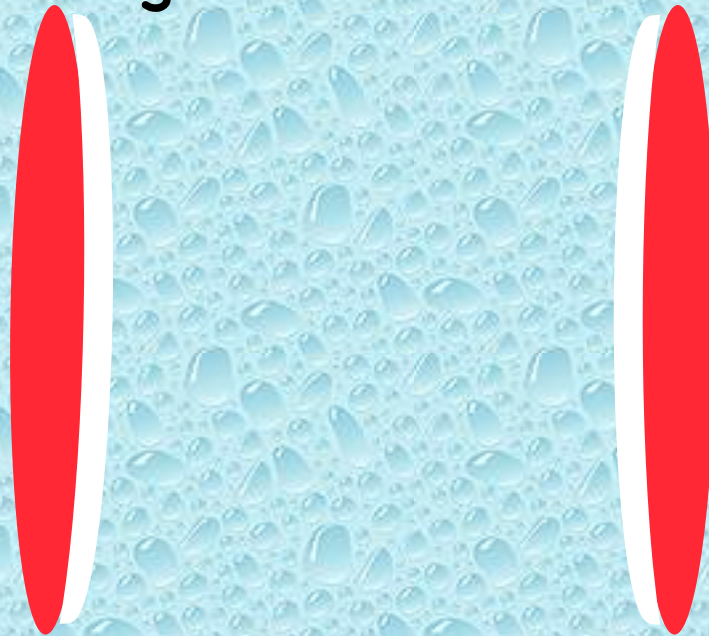
Water can not reorganize readily in the presence of a mesoscopically large hydrophobic interface, and therefore must break hydrogen-bonds to accommodate its presence



Hydrophobic plates  
modeled by  
Gay-Berne  
particles

# Hydrophobicity at Large Lengthscales

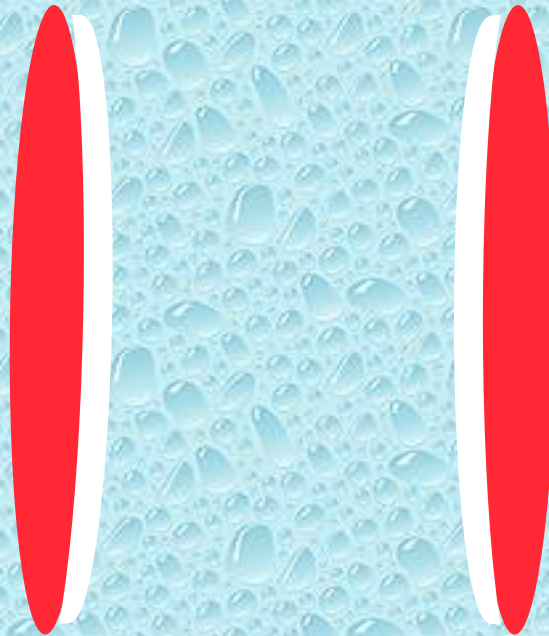
An “unbalancing” force develops near extended surfaces in which the solvent molecule pulls away from the interface with which it cannot gain favorable interactions



creating a thin vapor layer at surface to maximize interactions with the higher density phase. When there are a pair of such hydrophobic plates, two liquid-gas interfaces are formed

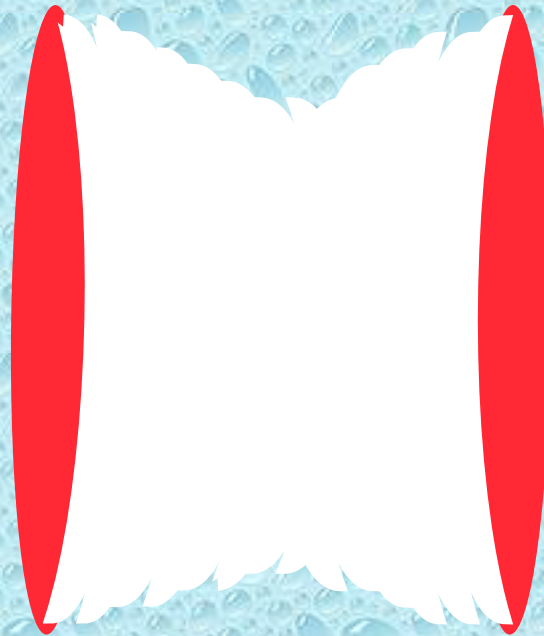
# Hydrophobicity at Large Lengthscales

Water will remain in the gap between the surfaces until a critical separation is reached,



# Hydrophobicity at Large Lengthscales

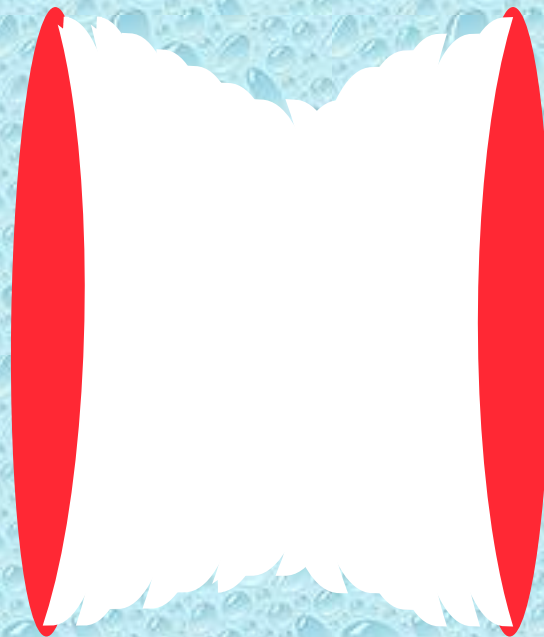
Water will remain in the gap between the surfaces until a critical separation is reached,



at which point the unfavorable interfacial energy is no longer compensated by the binding energy of the bulk liquid, and the liquid phase becomes metastable: it evaporates!

# Hydrophobicity at Large Lengthscales

Is water unique in its solvophobicity at large lengthscales?



Does the hydrogen-bonded network structure matter?



# Hydrophobicity at Large Lengthscales

If any amount of attraction exists between the GB particles and any of the liquids, no dewetting transition is observed



This means that the phenomena matters for materials that are very solvophobic- which we treat as repulsive GB particles

# Dewetting transitions for water-like liquids

Apparently altered interactions and hence networks can dewet, more or less efficiently, like water

H30 dewets  
at separation  
of 9A

SPC/E dewets  
at separation  
of 12A

B60 dewets  
at separation  
of 14A

# Dewetting transitions for water-like liquids

Apparently altered interactions and hence networks can dewet, more or less efficiently, like water

H30 dewets  
at separation  
of 9A

SPC/E dewets  
at separation  
of 12A

B60 dewets  
at separation  
of 14A

Can we determine what properties matter to predict the critical separations,  $D_c$ , at which a liquid will cavitate?

# Surface tensions and interface profiles

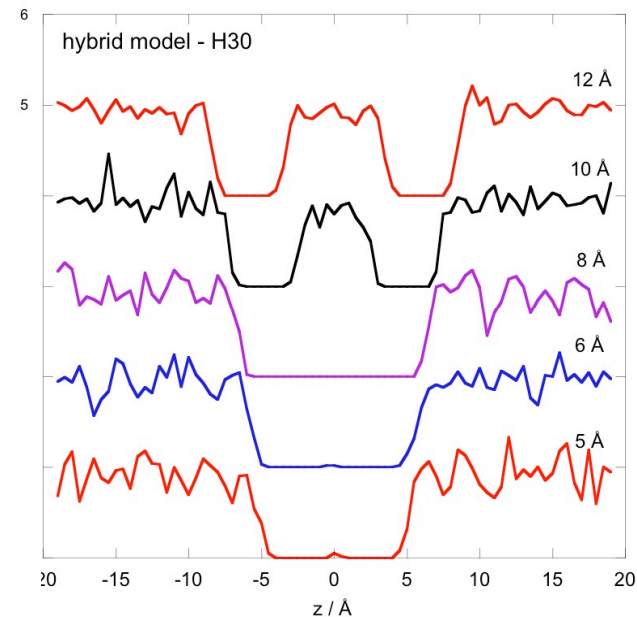
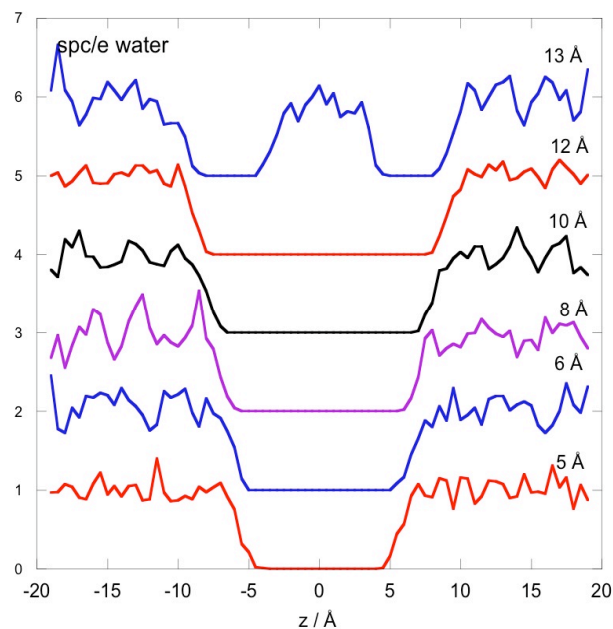
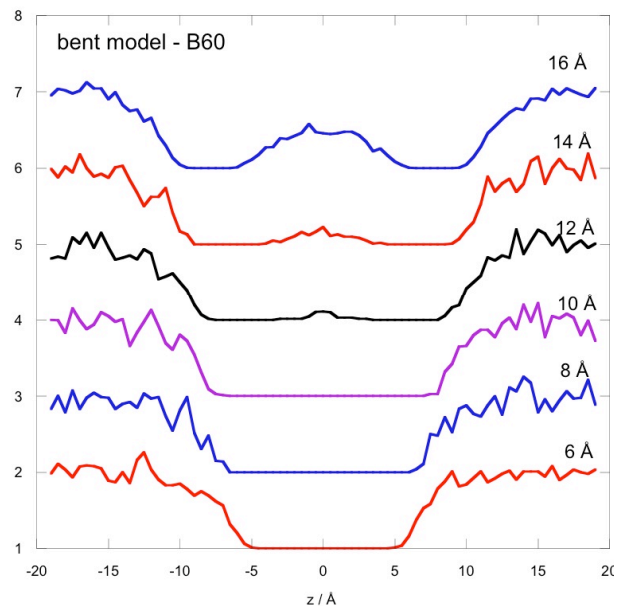
---

B60 (20 dyn/cm) < SPC/E (61 dyn/cm) < H30 (88 dyn/cm)

Head-Gordon & Lynden-Bell (2008). *JCP*

# Surface tensions and interface profiles

B60 (20 dyn/cm) < SPC/E (61 dyn/cm) < H30 (88 dyn/cm)



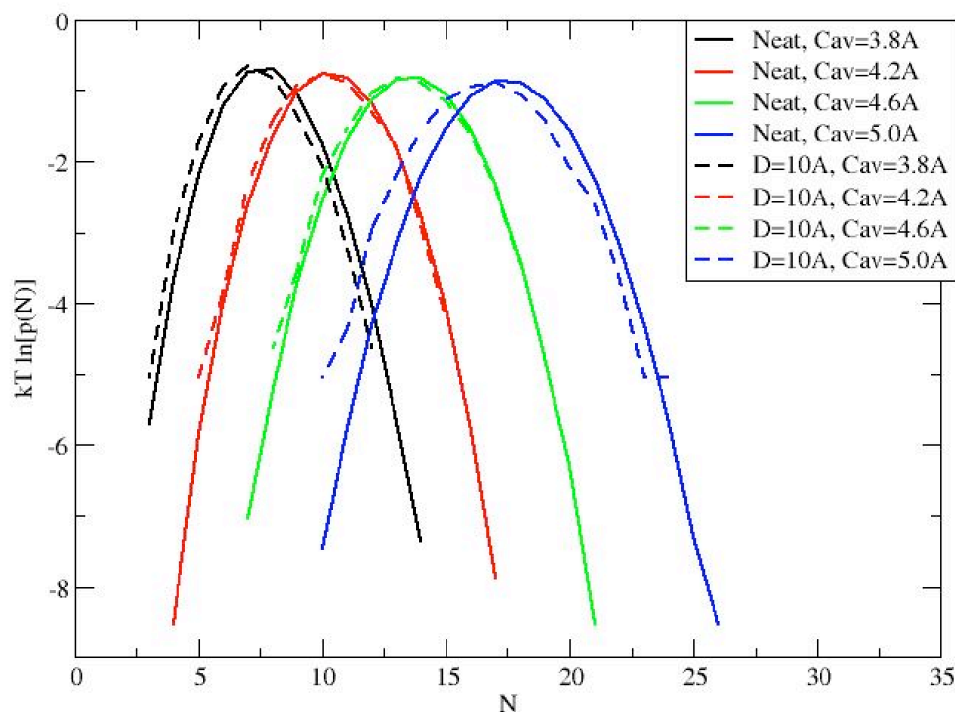
Interface is tighter for H30 like its greater solvophobicity for small hydrophobic solutes

Head-Gordon & Lynden-Bell (2008). *JCP*

# H3O density fluctuations

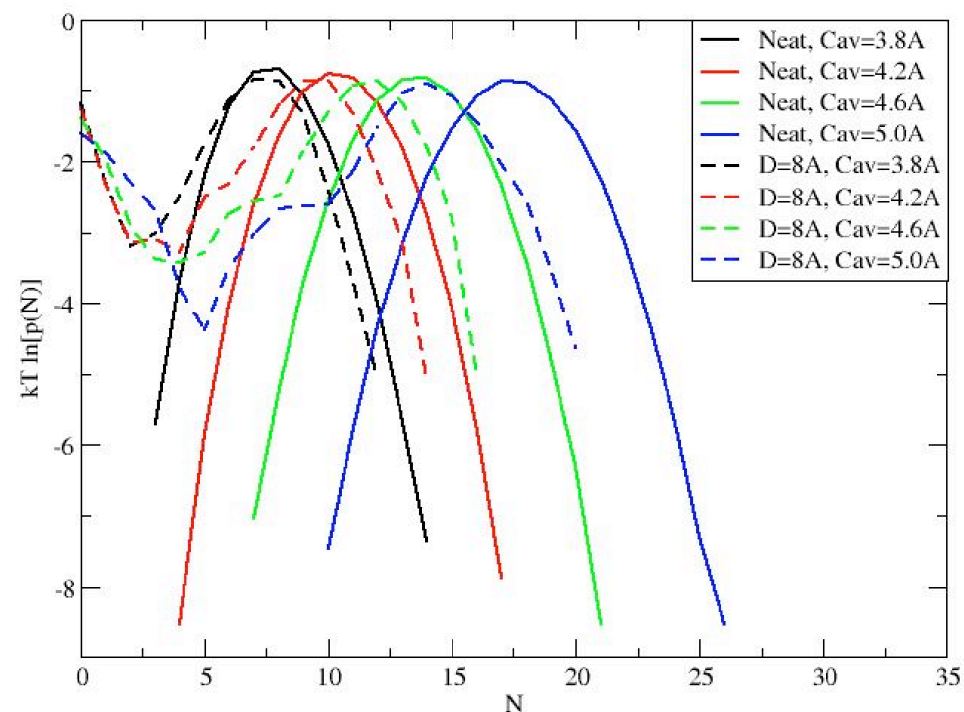
The water molecules in the center of the cavity between GB Hphobes obey Gaussian statistics like the neat liquid before the "Transition State" for the H3O liquid

H3O GB and Neat



$D > D_c$

H3O GB and Neat

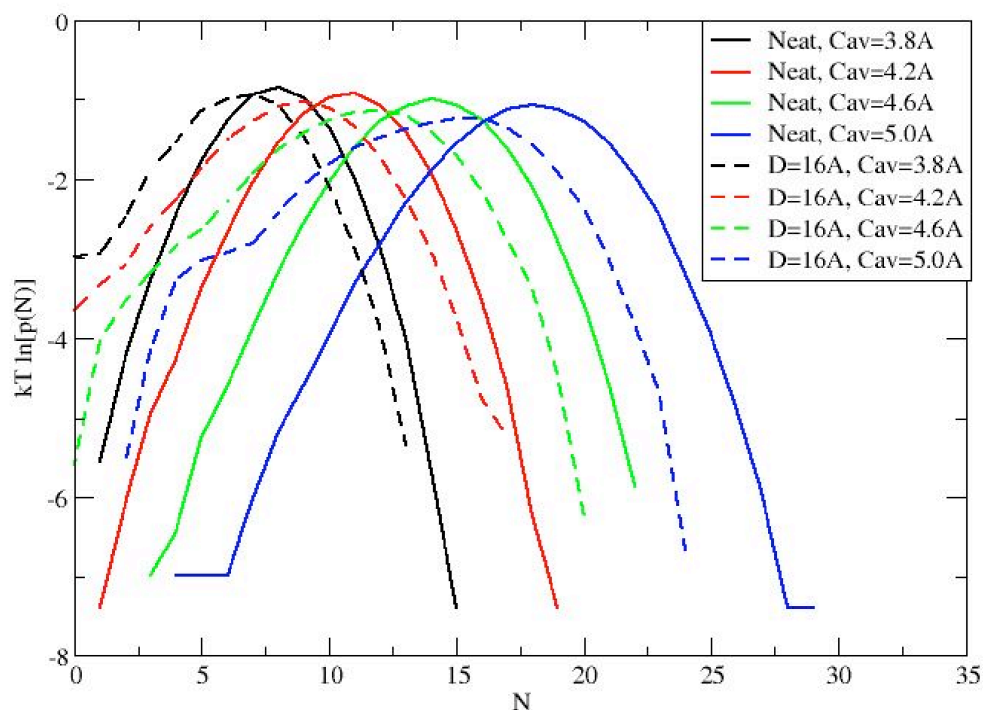


$D = D_c^*$

# B60 density fluctuations

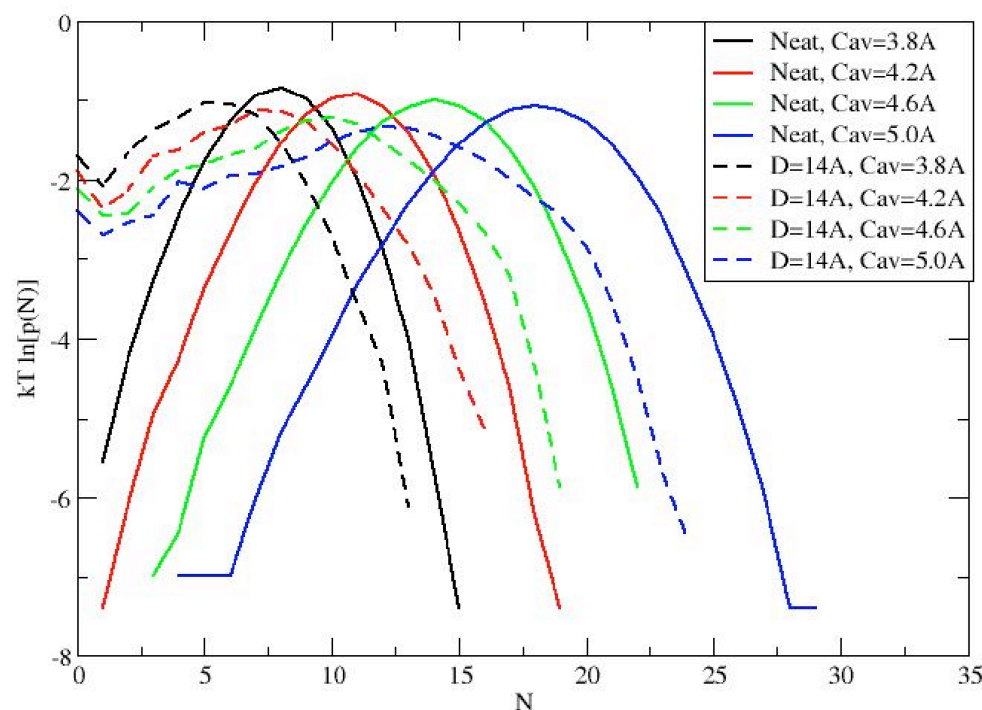
The water molecules in the center of the cavity between GB Hphobes DO NOT obey Gaussian statistics before the "Transition State" for the B60 liquid

B60 GB and Neat



$D > D_c$

B60 GB and Neat



$D = D_c^*$

# Correlation Lengths in Liquids

---

Egelstaff and Widom made the observation that the product of the surface tension ( $\gamma$ ) and the isothermal compressibility ( $\kappa$ ), with dimensions of length, was largely invariant over wide range of metallic, non-metallic liquids in coexistence with their vapor.



# Correlation Lengths in Liquids

---

Egelstaff and Widom made the observation that the product of the surface tension ( $\gamma$ ) and the isothermal compressibility ( $\kappa$ ), with dimensions of length, was largely invariant over wide range of metallic, non-metallic liquids in coexistence with their vapor.

The correlation length needed to reach bulk thermodynamics in either phase was derived by Widom to be:  $L = \gamma\kappa / 0.07$

# Correlation Lengths in Liquids

---

Egelstaff and Widom made the observation that the product of the surface tension ( $\gamma$ ) and the isothermal compressibility ( $\kappa$ ), with dimensions of length, was largely invariant over wide range of metallic, non-metallic liquids in coexistence with their vapor.

The correlation length needed to reach bulk thermodynamics in either phase was derived by Widom to be:  $L = \gamma\kappa / 0.07$

This implied that the liquid-gas interface is “sharp” on a macroscopic scale, invariant to liquid type, since this length varied by only 3–6Å

# Correlation Lengths in Liquids

---

Egelstaff and Widom made the observation that the product of the surface tension ( $\gamma$ ) and the isothermal compressibility ( $\kappa$ ), with dimensions of length, was largely invariant over wide range of metallic, non-metallic liquids in coexistence with their vapor.

The correlation length needed to reach bulk thermodynamics in either phase was derived by Widom to be:  $L = \gamma\kappa/0.07$

This implied that the liquid-gas interface is "sharp" on a macroscopic scale, invariant to liquid type, since this length varied by only 3-6Å

Isothermal compressibility:

H30 (25 atm<sup>-1</sup>) < SPC/E (52 atm<sup>-1</sup>) < B60 (231 atm<sup>-1</sup>)

Surface tension

B60 (20 dyn/cm) < SPC/E (61 dyn/cm) < H30 (88 dyn/cm)

# Liquid Correlation Lengths and Dewetting?

However this correlation length change will matter on the microscopic or mesoscopic lengthscales of our confined system. In our fluids, the Egelstaff-Widom length varies over this full 3-6Å range

Correlation length  $L$   
H30 (3.1Å) < SPC/E (4.6Å) < B60 (6.7Å)

High compressibility, low surface tension liquids can nucleate low density voids at the GB surface and cross to other GB surface

EW correlation length predicts dewetting trend

Head-Gordon & Lynden-Bell (2008). *JCP*

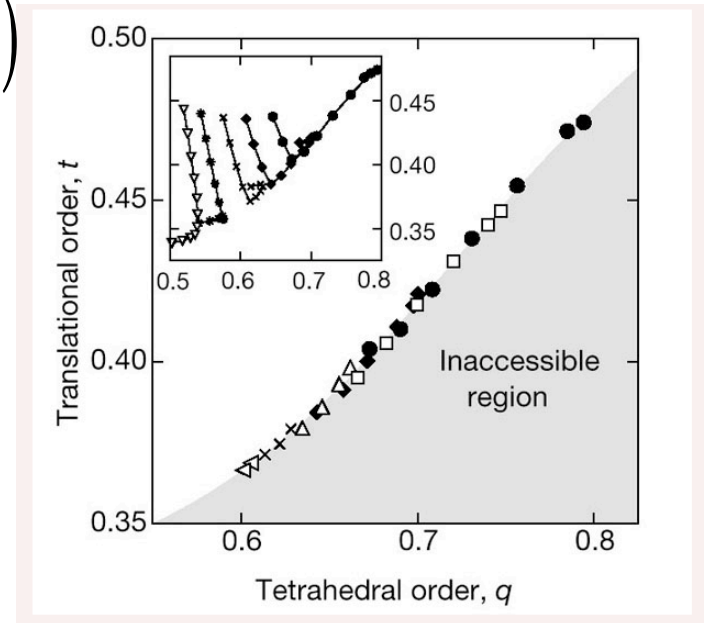
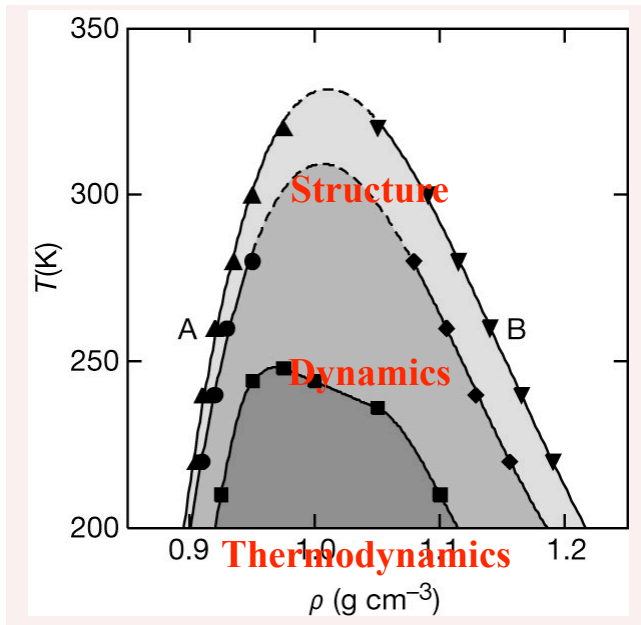
# Anomalies in Bulk Supercooled Water

Orientational order,  $q$

$$q = 1 - \frac{3}{8} \sum_{j=1}^3 \sum_{k=j+1}^4 \left( \cos \psi_{jk} + \frac{1}{3} \right)^2$$

Translational order,  $t$

$$t = \frac{\int_0^{r_c} |g(r) - 1| dr}{r_c}$$



Errington and Debenedetti (2001). *Nature*.

Where  $q$  and  $t$  extrema are tightly coupled defines structural anomalous region, signaling cascade of diffusion and thermodynamic anomalies

Connection between dynamical and thermodynamic anomalies?

Lecture 2

# Isotropic Water Potential: Two Lengthscales

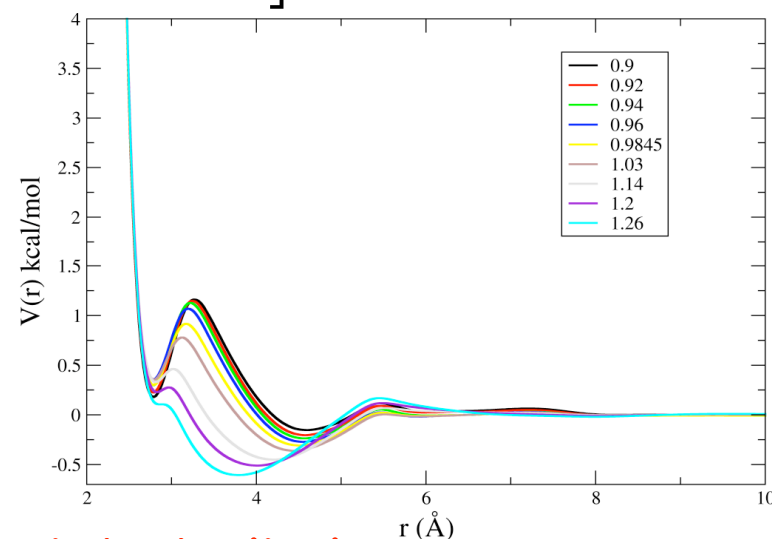
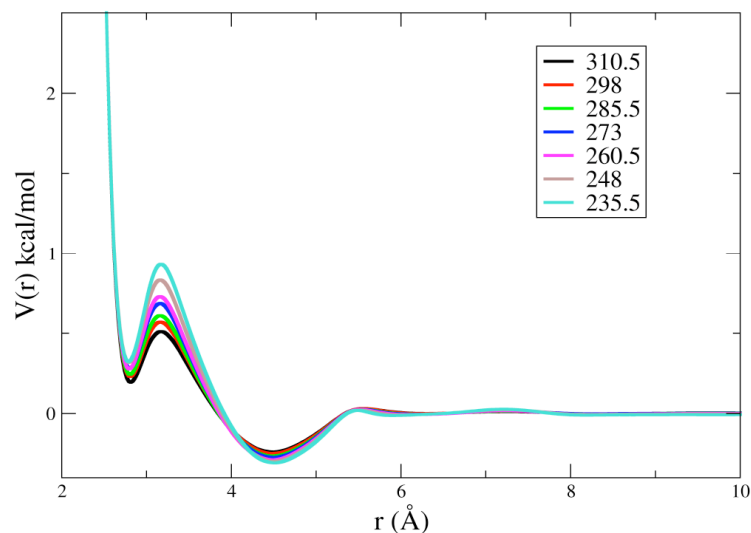
Integral equation provides reference potential, and numerical procedure gives *unique* potential that reproduces (TIP4P-EW)  $g_{OO}(r)$  exactly.

$$V_g^{ISO}(r) = V_g^{OZ/HNC}(r) + kT \ln \left[ \frac{g_{OO}^{ISO}(r)}{g_{OO}^{TIP4PEW}(r)} \right]$$

# Isotropic Water Potential: Two Lengthscales

Integral equation provides reference potential, and numerical procedure gives *unique* potential that reproduces (TIP4P-EW)  $g_{OO}(r)$  exactly.

$$V_g^{ISO}(r) = V_g^{OZ/HNC}(r) + kT \ln \left[ \frac{g_{OO}^{ISO}(r)}{g_{OO}^{TIP4PEW}(r)} \right]$$



This is done at each state point studied.

Loss of explicit hydrogen-bonding

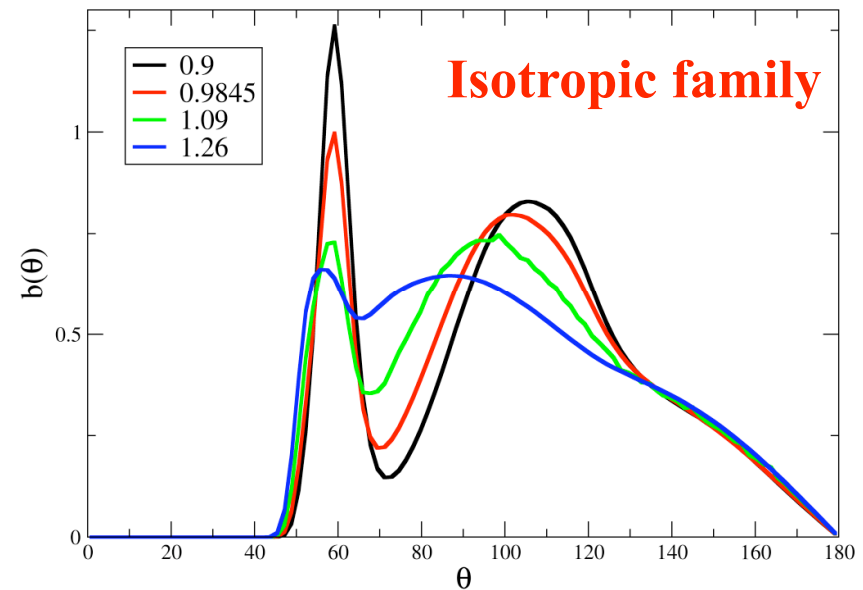
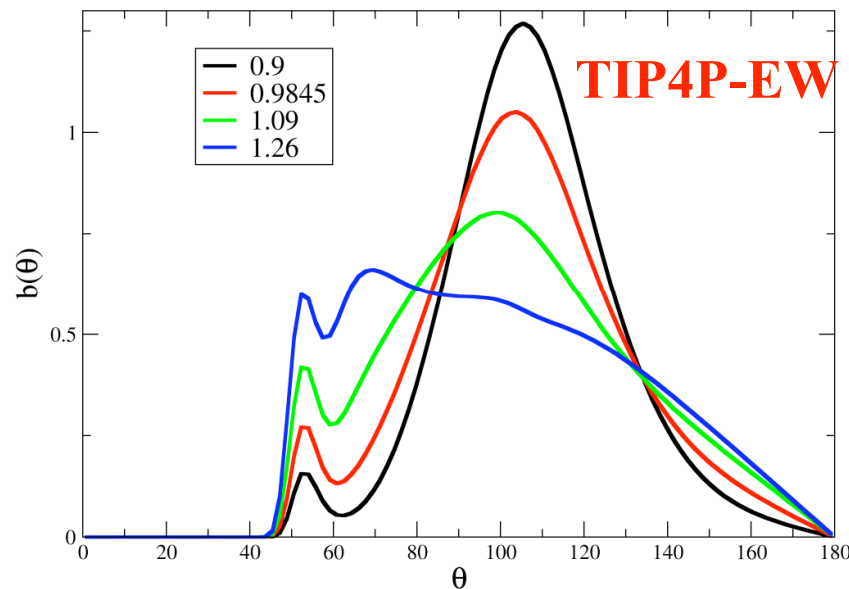
Translational order,  $t$ , is exact by construction

Johnson, THG, Louis (2007). *JCP* 126, 144509

# Structural Order (not Tetrahedral order) is Anomalous

Two body correlations correct by construction,  
but what does local three body order look like?

$$b(\theta) = \int_0^{R_c} dr_{12} \int_0^{R_c} dr_{13} g_3(r_{12}, r_{13}, \theta) r_{12}^2 r_{13}^2$$

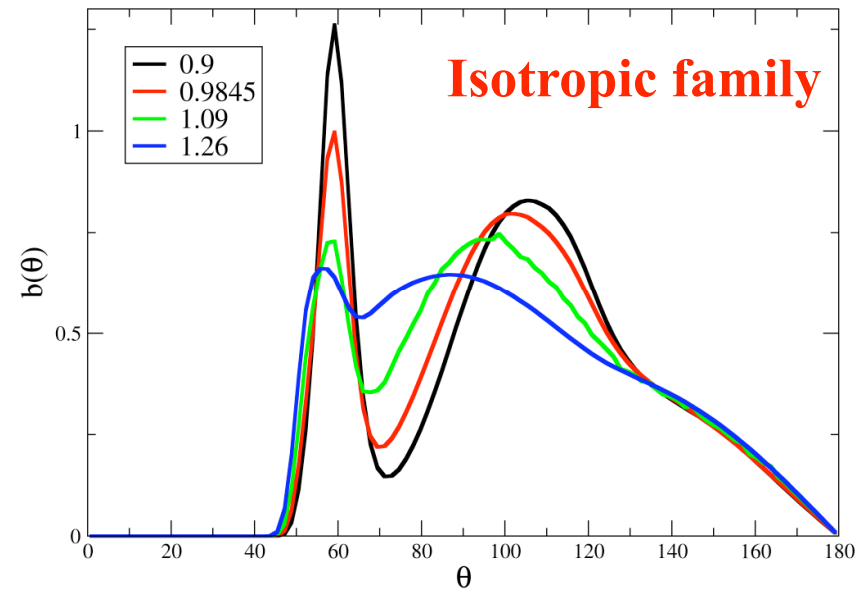
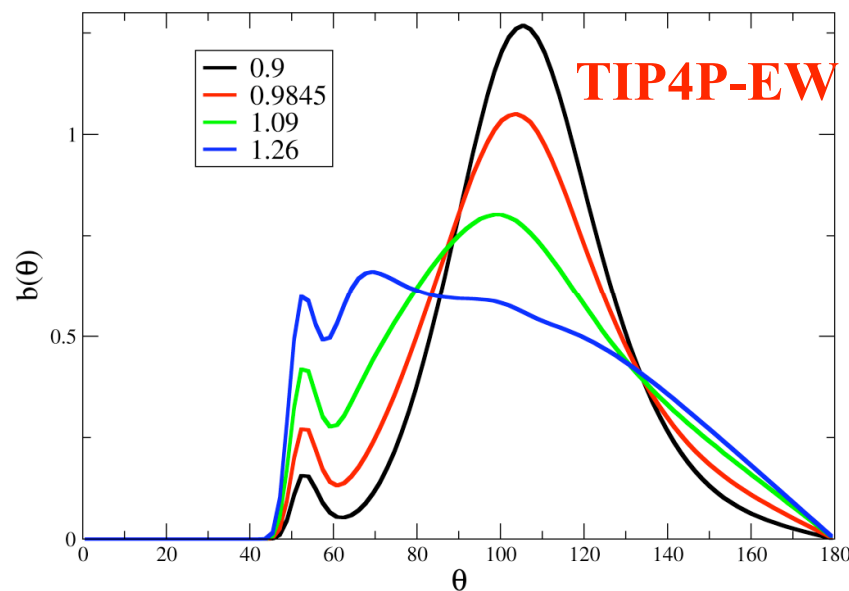




# Structural Order (not Tetrahedral order) is Anomalous

Two body correlations correct by construction,  
but what does local three body order look like?

$$b(\theta) = \int_0^{R_c} dr_{12} \int_0^{R_c} dr_{13} g_3(r_{12}, r_{13}, \theta) r_{12}^2 r_{13}^2$$



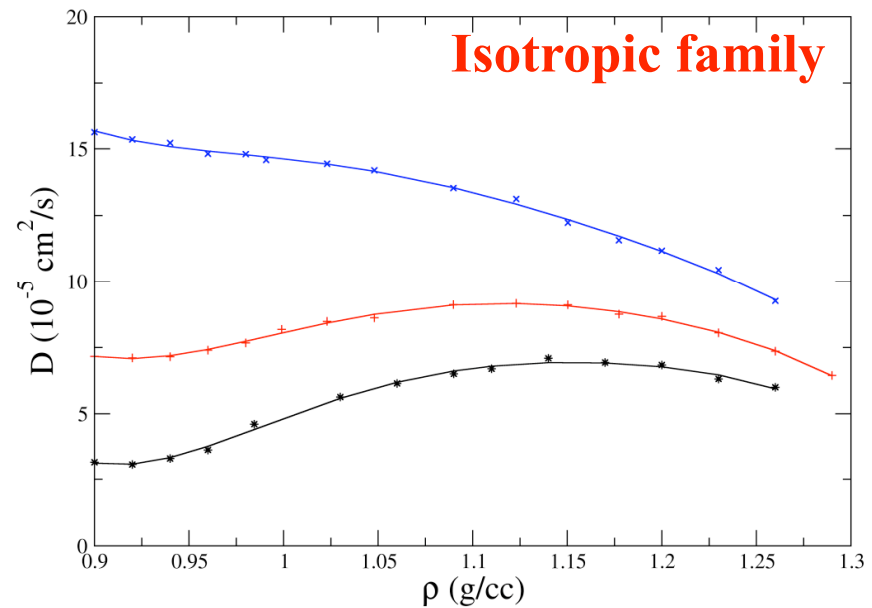
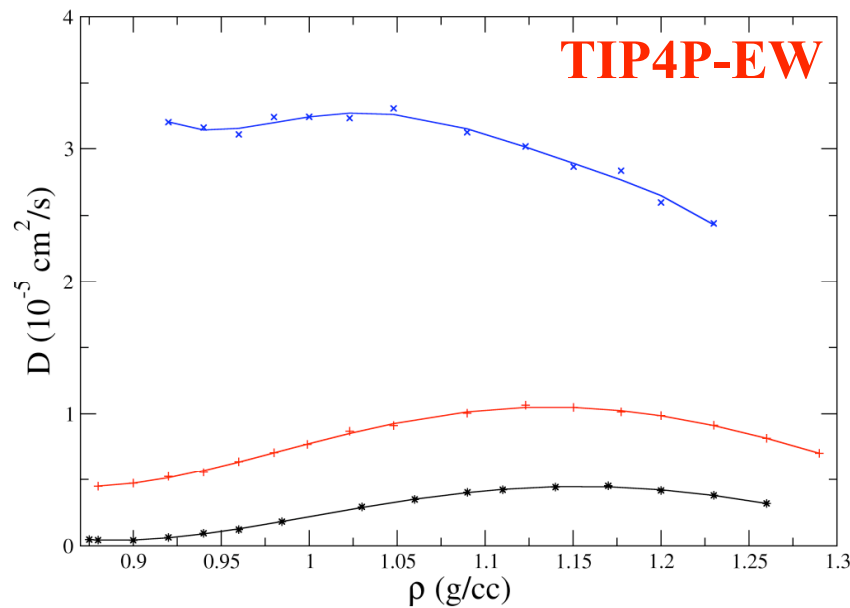
While  $q$  does not decrease with compression for isotropic, *local* three body order metric does show anomalous behavior

Johnson, Louis, Head-Gordon (2007). *JCP* 126, 144509

# Dynamic Anomalies Show Almost Quantitative Density Dependence

While  $D_{\text{trans}}$  for isotropic family are  $\sim 5$  times faster, they show diffusion maxima, minima at same  $\rho$  as reference potential

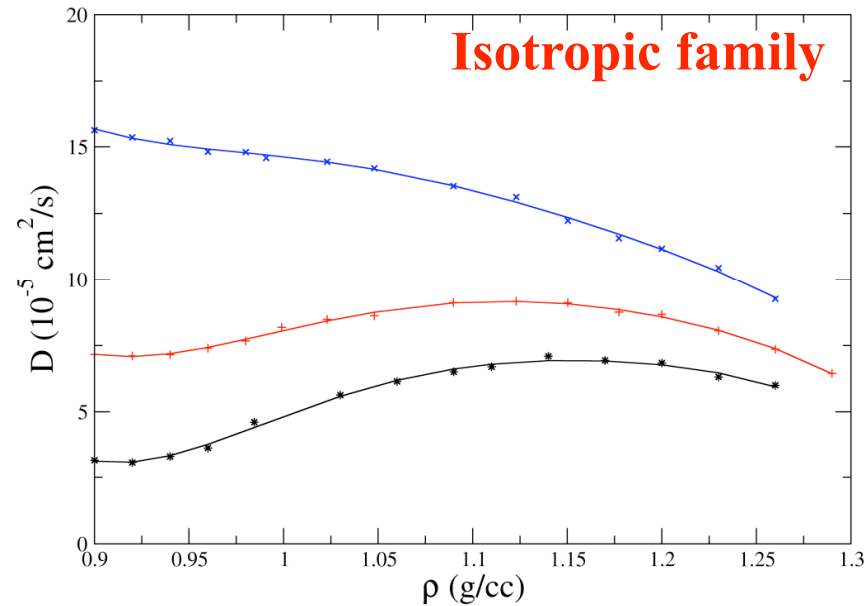
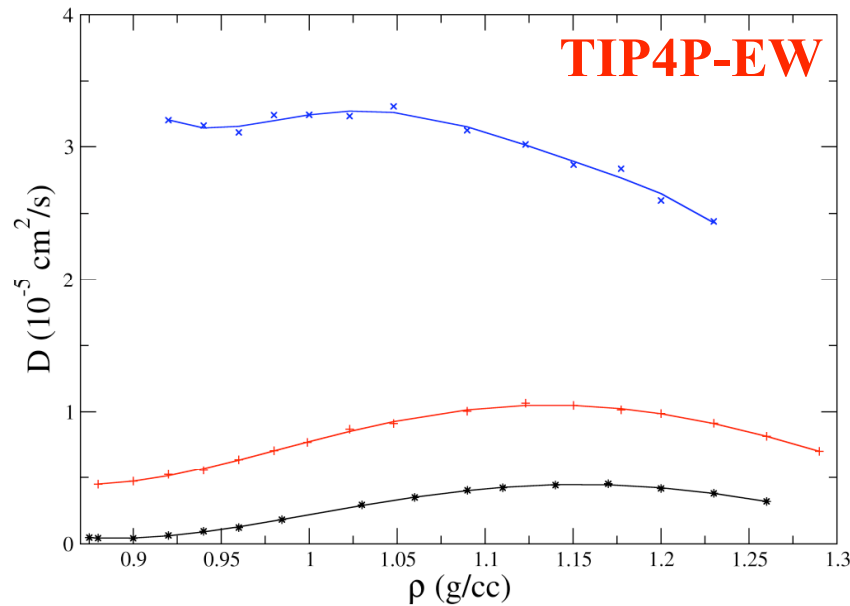
310  
260  
235



# Dynamic Anomalies Show Almost Quantitative Density Dependence

While  $D_{\text{trans}}$  for isotropic family are  $\sim 5$  times faster, they show diffusion maxima, minima at same  $\rho$  as reference potential

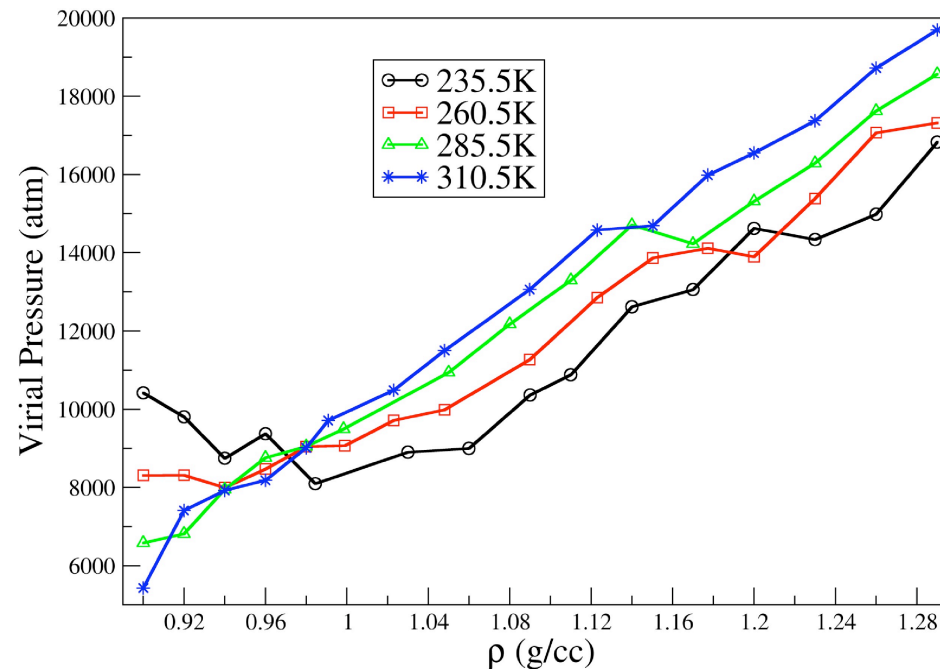
310  
260  
235



Diffusive maxima occur at minimum order in  $f$   
Diffusive minima occur at maximum order in  $b(\theta)$ , but not  $q$ !

# No Evidence of Thermodynamic Anomalies

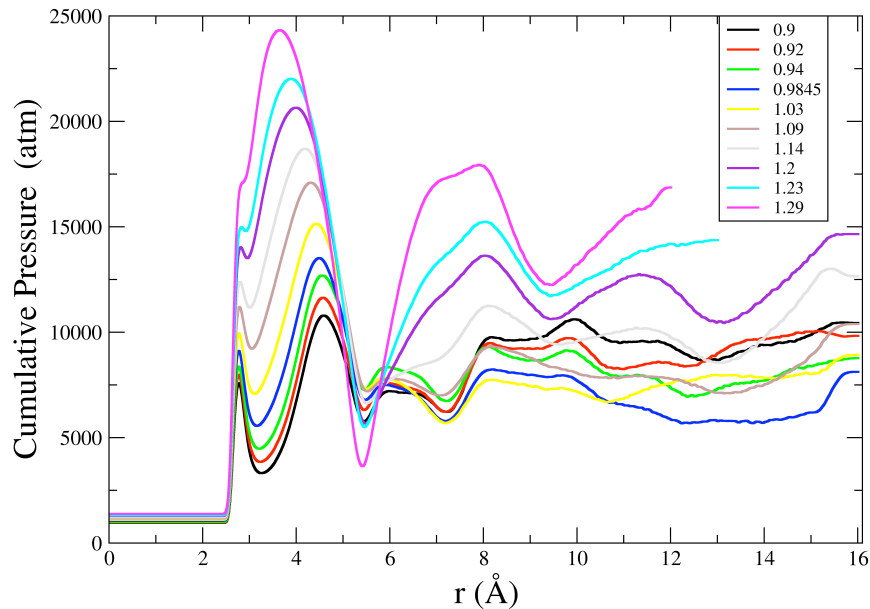
Density maxima criteria would satisfy:  $\left. \frac{d\rho}{dT} \right|_P > 0$



Is not consistently satisfied by Isotropic family, but cycles in and out of exhibiting a thermodynamic anomaly

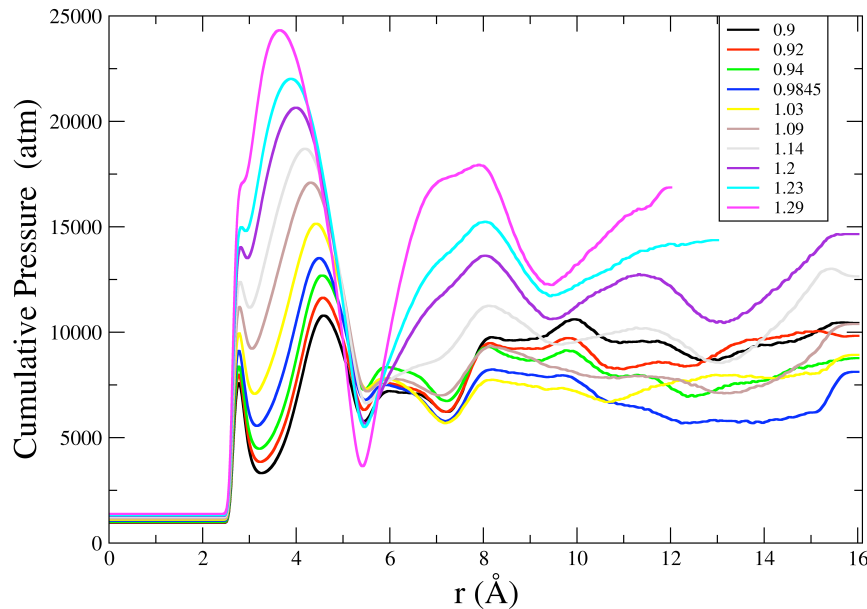
Johnson, THG, Louis (2007). *JCP* 126, 144509-144519

# Thermodynamic Consistency is Only Realized over Short Range



Reproducing  $g_{OO}(r)$  gives enough local (defective) tetrahedral order to manifest diffusion anomaly, but local defects contribute to lack of coherence in long-range order so that expansion on cooling cannot be supported

# Thermodynamic Consistency is Only Realized over Short Range



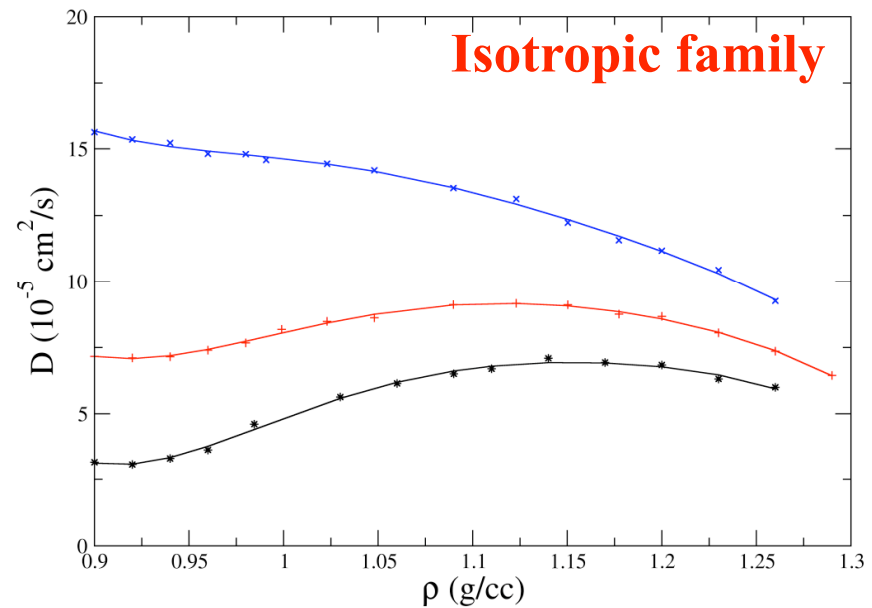
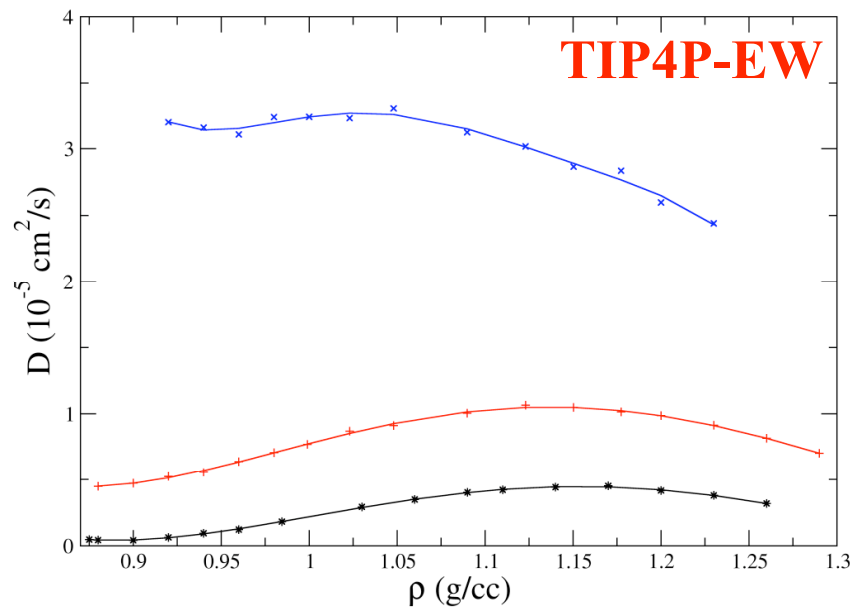
Reproducing  $g_{OO}(r)$  gives enough local (defective) tetrahedral order to manifest diffusion anomaly, but local defects contribute to lack of coherence in long-range order so that expansion on cooling cannot be supported

Dynamic anomalies only need local structural order while thermodynamic anomalies require long-range tetrahedral order

# Dynamic Anomalies Show Almost Quantitative Density Dependence

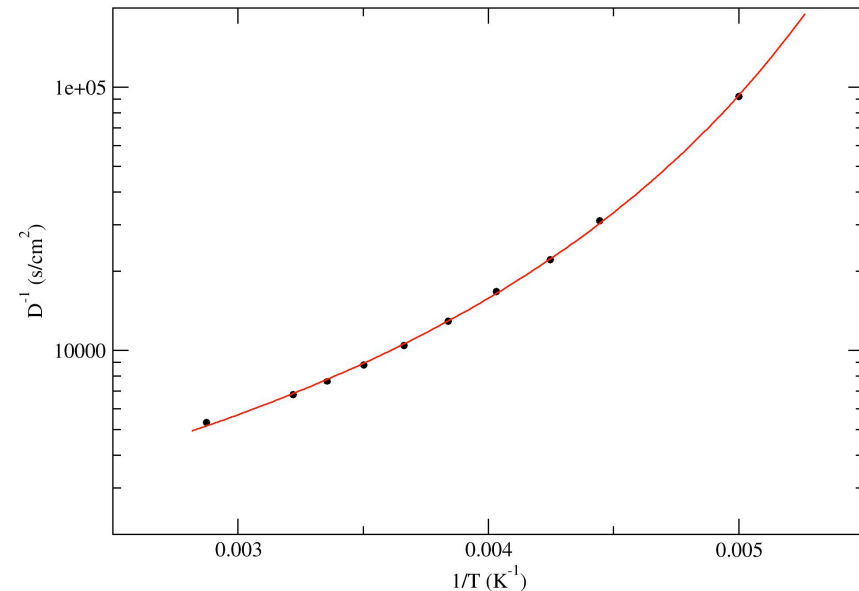
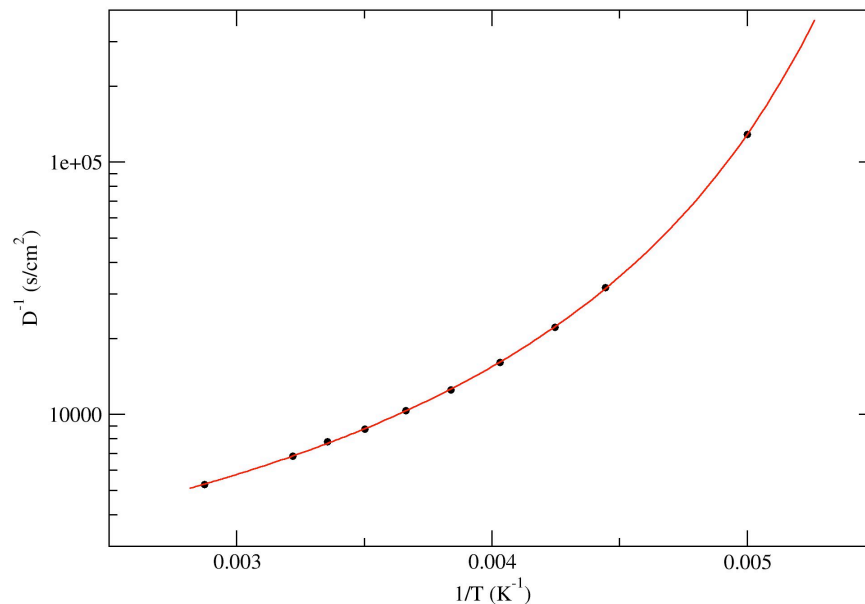
While  $D_{\text{trans}}$  for isotropic family are  $\sim 5$  times faster, they show diffusion maxima, minima at same  $\rho$  as reference potential

310  
260  
235



# Dynamics are also Fragile with Temperature

Whether family is investigated at constant pressure or density, the temperature dependence of dynamics is non-Arrhenius



Well fit to the VFT functional form.

$$D_t(T) = D_0 \exp\left(\frac{BT_0}{T - T_0}\right)$$



# Adams-Gibbs Theory

---

The Adams-Gibbs relation provides an explicit connection between the temperature dependence of translational diffusion and the configurational entropy,  $S_c$ , through the relation

$$D_t = D_0 \exp\left(\frac{A}{TS_c}\right)$$

where  $D_0$  and  $A$  are assumed to be *temperature-independent* constants.

# Adams-Gibbs Theory

---

The Adams-Gibbs relation provides an explicit connection between the temperature dependence of translational diffusion and the configurational entropy,  $S_c$ , through the relation

$$D_t = D_0 \exp\left(\frac{A}{TS_c}\right)$$

where  $D_0$  and  $A$  are assumed to be *temperature-independent* constants.

$S_c$  has been empirically related to observed trends of heat capacity and temperature [Angell]

$$S_c \approx \int_{T_0}^T \frac{\Delta C_p}{T'} dT' \approx \int_{T_0}^T \frac{A'}{T'^2} dT' = A' \left( \frac{1}{T_0} - \frac{1}{T} \right)$$

# Adams-Gibbs Theory

---

By substituting

$$S_c \approx \int_{T_0}^T \frac{\Delta C_p}{T'} dT' \approx \int_{T_0}^T \frac{A'}{T'^2} dT' = A' \left( \frac{1}{T_0} - \frac{1}{T} \right)$$

Into

$$D_t = D_0 \exp\left(\frac{A}{TS_c}\right)$$

we recover the VFT functional form, known to fit experimental transport properties well over a large temperature range.

# Adams-Gibbs Theory

---

By substituting

$$S_c \approx \int_{T_0}^T \frac{\Delta C_p}{T'} dT' \approx \int_{T_0}^T \frac{A'}{T'^2} dT' = A' \left( \frac{1}{T_0} - \frac{1}{T} \right)$$

Into

$$D_t = D_0 \exp\left(\frac{A}{TS_c}\right)$$

we recover the VFT functional form, known to fit experimental transport properties well over a large temperature range.

Thus a linear correlation between  $\ln D_t$  and  $S_c$  is expected from their observed experimental trends with temperature

# Correlations with excess entropy

Dzugutov (Nature 2001) noted a relationship between a scaled diffusion constant,  $D^*$ , and excess entropy with respect to an ideal gas

$$D^* = D_0^* \exp(\alpha S_{excess})$$

or with  $S_{excess} \sim S_2$  (pair correlations only)

$$S_{excess} \approx S_2 = -2\pi\rho \int_0^\infty \left\{ g(r) \ln g(r) - [g(r) - 1] \right\} r^2 dr$$

$D_0^*$  and  $\alpha$  are universal constants. Because it is postulated to be a universal scaling law, it should hold for this family of potentials if it is accurate.

# Thermodynamic and Dynamic Relations

For A-G theory and Dzugutov universal scaling, suggests that the calculation of the partition function is all that is needed to predict transport properties and not time-evolved configurations

# Thermodynamic and Dynamic Relations

For A-G theory and Dzugutov universal scaling, suggests that the calculation of the partition function is all that is needed to predict transport properties and not time-evolved configurations

With A-G we explore whether the diminishing configuration count of  $S_c$  is predictive of  $D_{trans}$ , but by removing a common potential energy surface and expected temperature trends

# Thermodynamic and Dynamic Relations

For A-G theory and Dzugutov universal scaling, suggests that the calculation of the partition function is all that is needed to predict transport properties and not time-evolved configurations

With A-G we explore whether the diminishing configuration count of  $S_c$  is predictive of  $D_{trans}$ , but by removing a common potential energy surface and expected temperature trends

With Dzugutov universal scaling, we explore whether a different configuration count of  $S_{excess}$  is predictive of  $D_{trans}$



# Thermodynamic and Dynamic Relations

For A-G theory and Dzugutov universal scaling, suggests that the calculation of the partition function is all that is needed to predict transport properties and not time-evolved configurations

With A-G we explore whether the diminishing configuration count of  $S_c$  is predictive of  $D_{trans}$ , but by removing a common potential energy surface and expected temperature trends

With Dzugutov universal scaling, we explore whether a different configuration count of  $S_{excess}$  is predictive of  $D_{trans}$

Each thermodynamic and dynamic quantity at each state point is calculated by a different isotropic potential derived to reproduce  $g_{OO}(r;p,T)$

# Adams-Gibbs Theory

---

To calculate configurational entropy, we need to subtract off the vibrational entropy, starting with harmonic

$$S_{\text{harmonic}}(T, \rho) = k_b \sum_{i=1}^{3N} \left[ 1 - \log \left( \frac{\omega_i}{k_b T} \right) \right]$$

# Adams-Gibbs Theory

To calculate configurational entropy, we need to subtract off the vibrational entropy, starting with harmonic

$$S_{harmonic}(T, \rho) = k_b \sum_{i=1}^{3N} \left[ 1 - \log \left( \frac{\omega_i}{k_b T} \right) \right]$$

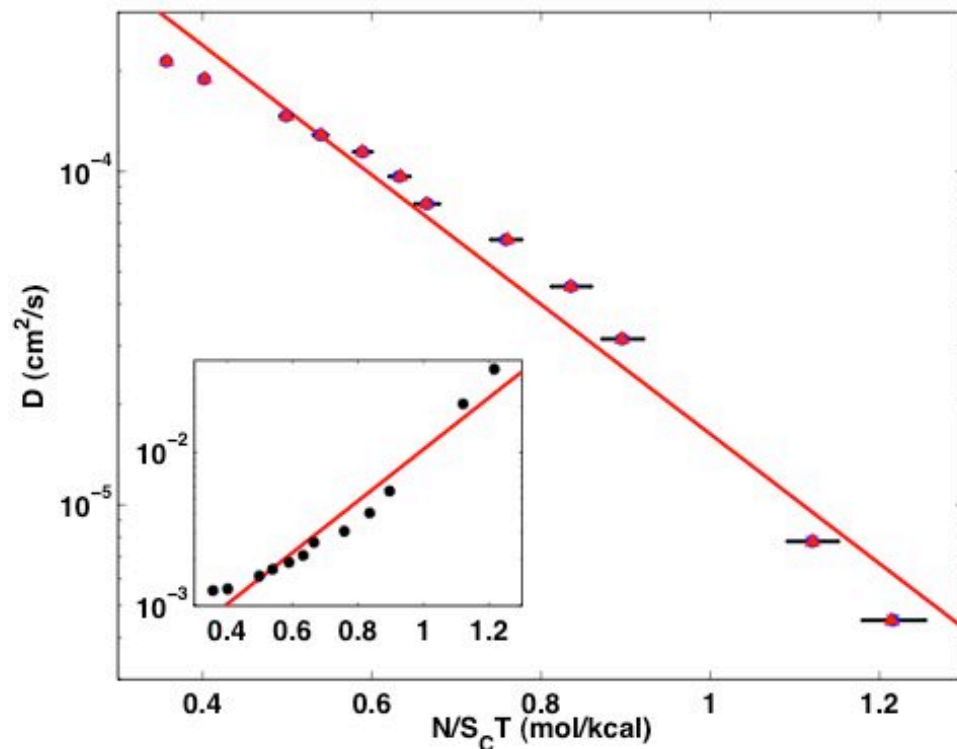
We found anharmonicity effects of ~10-20% for all state points investigated and therefore we always included an anharmonic correction of the form

$$S_{anharmonic}(T, \rho) = 2aT + \frac{3}{2}bT^2$$

# Adams-Gibbs Theory

To calculate configurational entropy, we need to subtract off the vibrational entropy, starting with harmonic

$$S_{harmonic}(T, \rho) = k_b \sum_{i=1}^{3N} \left[ 1 - \log \left( \frac{\omega_i}{k_b T} \right) \right]$$



We found anharmonicity effects of ~10-20% for all state points investigated and therefore we always included an anharmonic correction of the form

$$S_{anharmonic}(T, \rho) = 2aT + \frac{3}{2}bT^2$$

Johnson & Head-Gordon (2009). *JCP*

# Dynamical correlations with excess entropy

Using thermodynamic integration from the ideal gas, we

$$S_{tot}(T, \rho) = \frac{1}{T} \left( \langle U \rangle_{T, \rho} - \langle A \rangle_{T, \rho} \right)$$

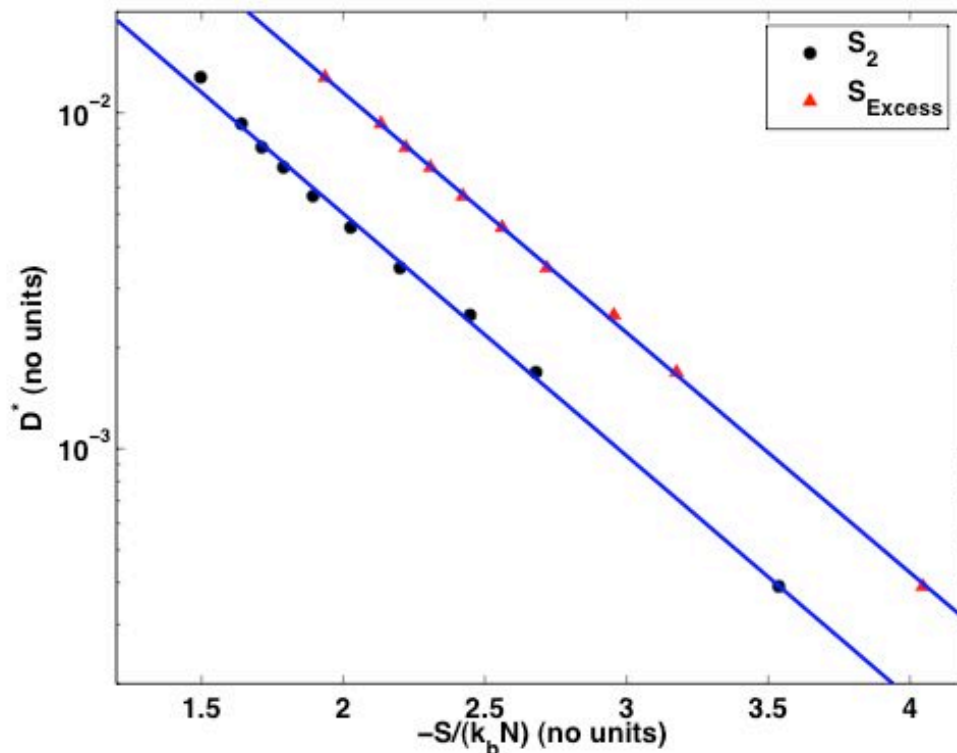
and subtract off ideal gas contribution to get  $S_{excess}$

# Dynamical correlations with excess entropy

Using thermodynamic integration from the ideal gas, we

$$S_{tot}(T, \rho) = \frac{1}{T} \left( \langle U \rangle_{T, \rho} - \langle A \rangle_{T, \rho} \right)$$

and subtract off ideal gas contribution to get  $S_{excess}$



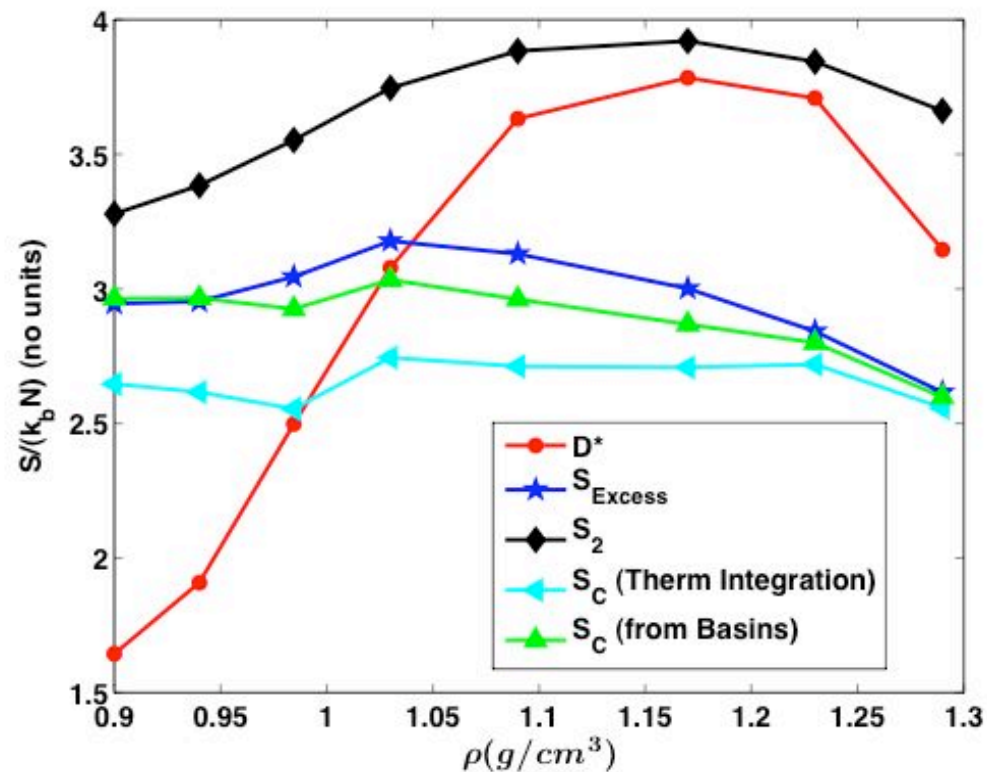
While  $D_0^*$  and  $\alpha$  are different than found by Dzugutov, the correlation of  $D^*$  with  $S_{excess}$  is perfect over full temperature range (down to 200K)

Johnson & Head-Gordon (2009). *JCP*

# Dynamical correlations with excess entropy

S<sub>2</sub> is the best correlator with Dt for dynamical anomalies with density

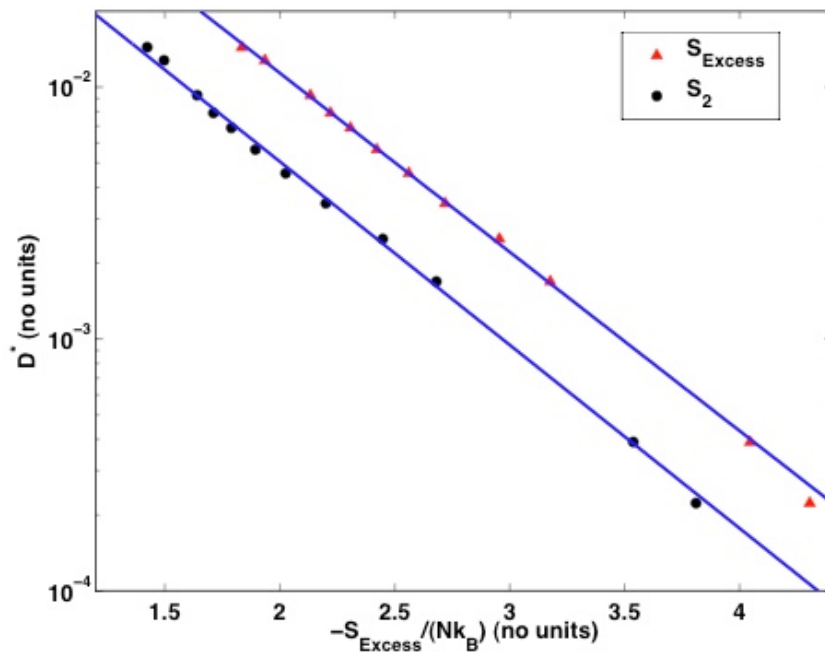
$$S_{\text{excess}} \approx S_2 = -2\pi\rho \int_0^{\infty} \left\{ g(r) \ln g(r) - [g(r) - 1] \right\} r^2 dr$$



Johnson & Head-Gordon (2009). *JCP*

# Thermodynamic-Dynamics for Deeply Supercooled States

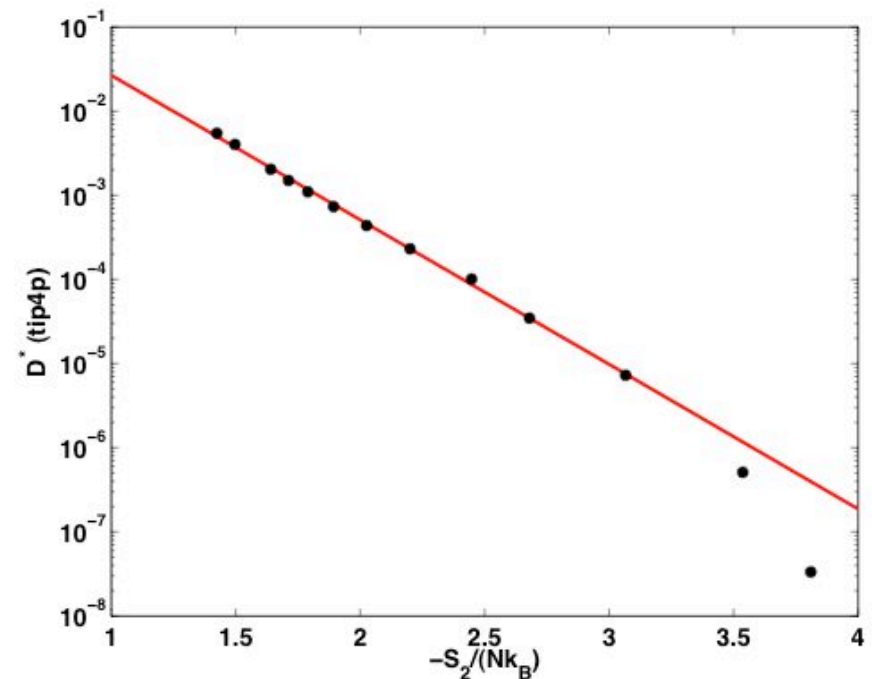
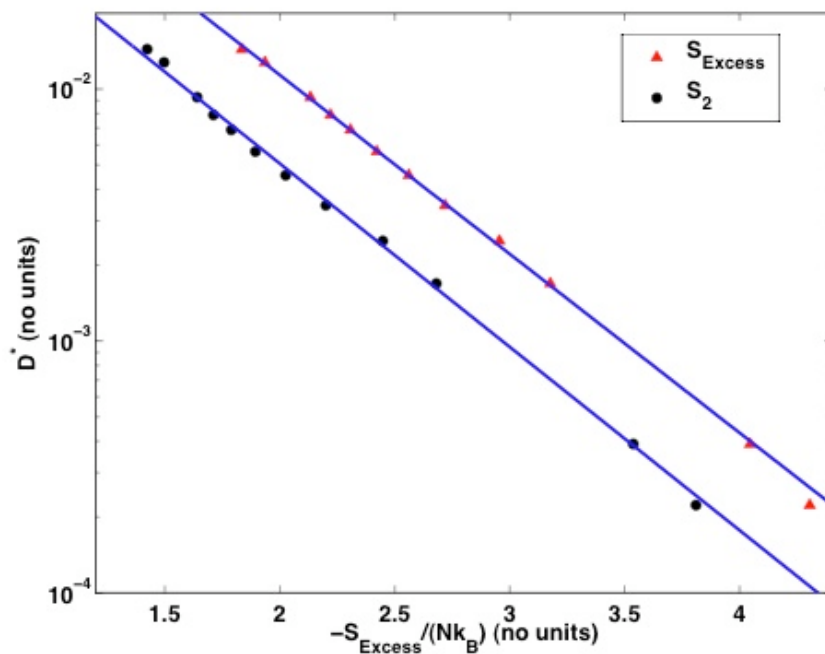
Relationship between  $D^*$  and  $S_2$  ( $S_{\text{Excess}}$ ) falters at 190K for family of potentials





# Thermodynamic-Dynamics for Deeply Supercooled States

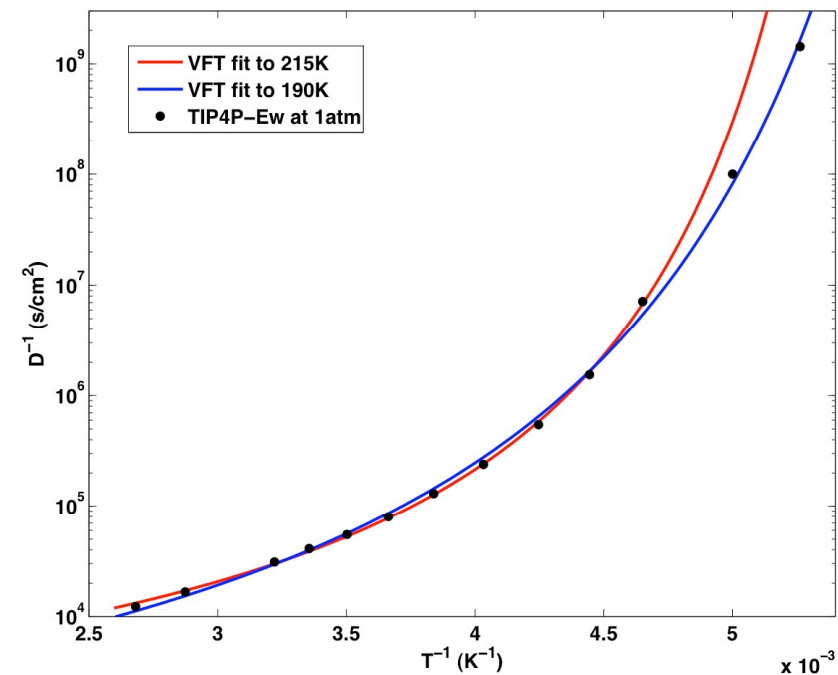
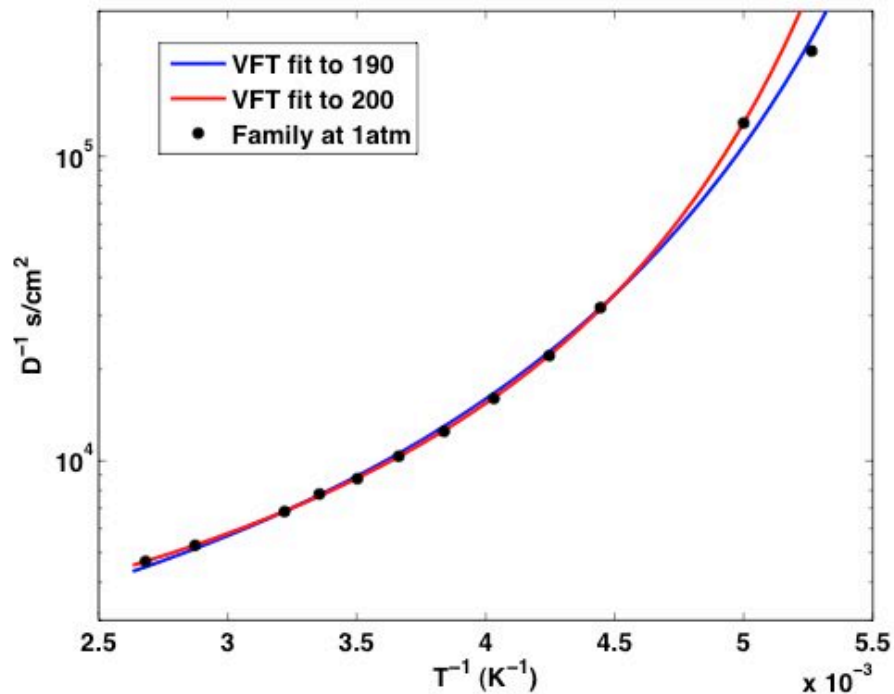
Relationship between  $D^*$  and  $S_2$  ( $S_{\text{Excess}}$ ) falters at 190K for family of potentials



$S_2$  same for complete water model by construction, but also fails at deeply supercooled temperatures (200K)

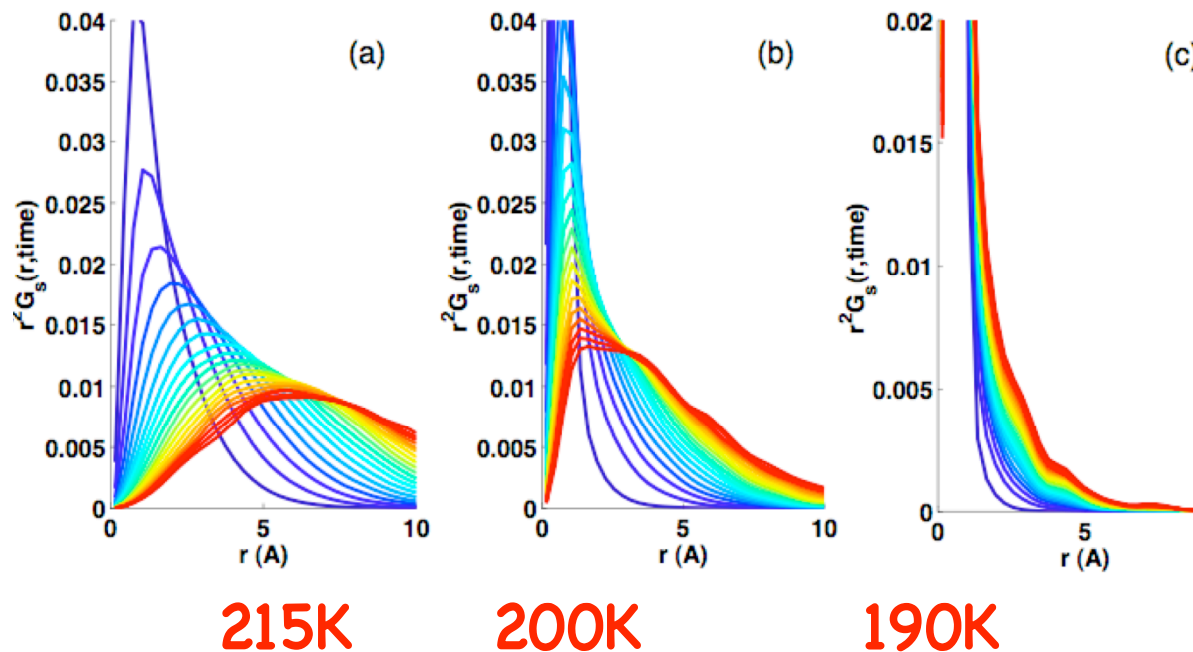
# Thermodynamic-Dynamic Relations Fail at Deeply Supercooled Temperatures

Neither family or complete water model conforms to a single acceptable VFT fit.



From fragile to less fragile (and maybe evidence for fragile to strong transition in water)

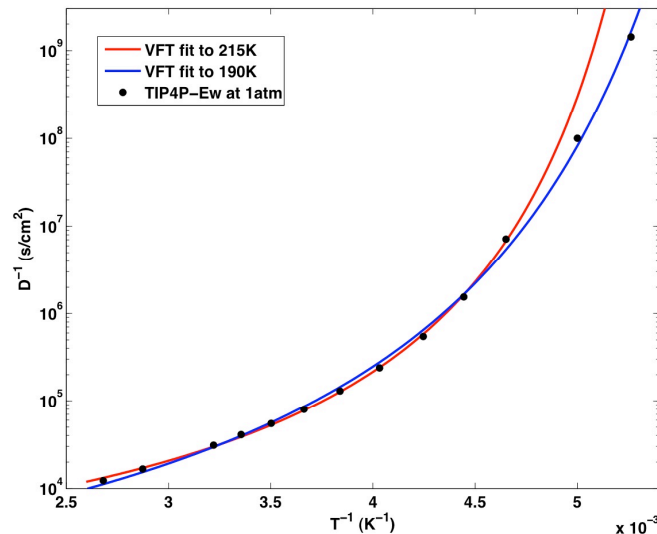
# Failure with Heterogeneous Dynamics



van Hove self correlation for particle displacements should approach Gaussian distribution at long time-scales

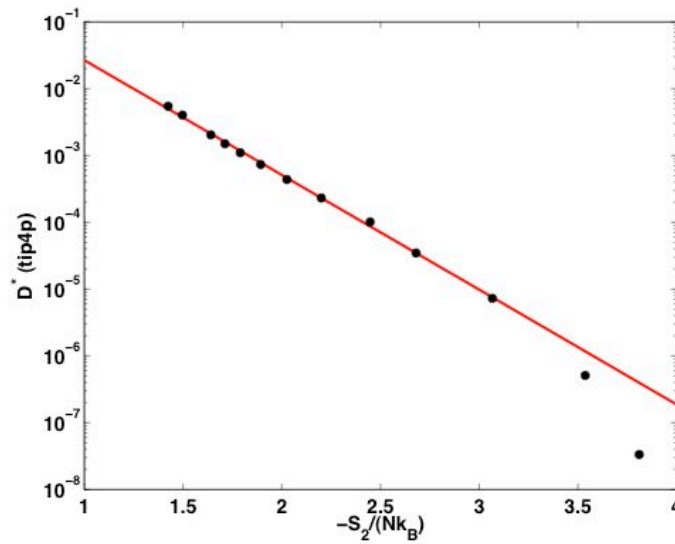
At temperatures where thermodynamic relations fail is when non-Gaussian distribution of displacements are observed- i.e. onset of heterogeneous dynamics

# Assessing Thermodynamic Theories for Liquid Dynamics



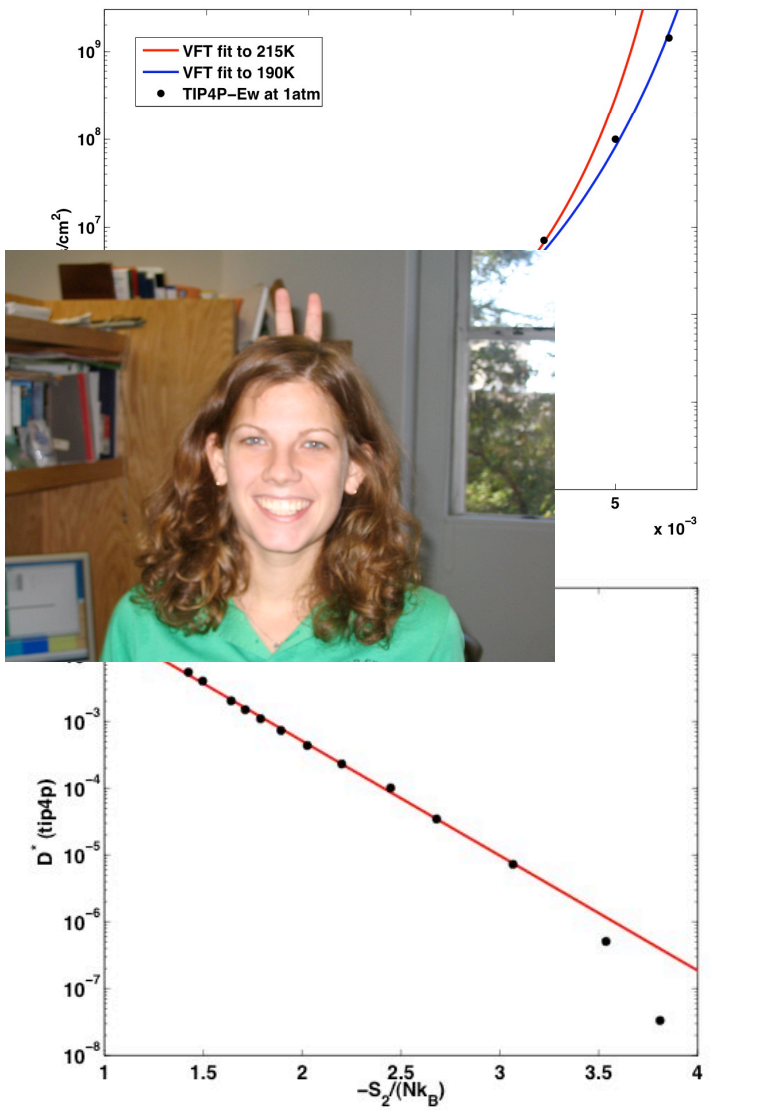
Accessible configurations captured in Sexcess or S2 diminish with temperature so that dynamics may be predicted for lightly supercooled states

However, the theories ultimately fail at the coldest temperatures where heterogeneous dynamics manifest



A theory that incorporates diffusive pathways through barriers, or describes higher order correlations, appear to be absolutely necessary

# Assessing Thermodynamic Theories for Liquid Dynamics



Accessible configurations captured in  $S_{\text{excess}}$  or  $S_2$  diminish with temperature so that dynamics may be predicted for lightly supercooled states

However, the theories ultimately fail at the coldest temperatures where glassy dynamics is most manifest

A theory that incorporates diffusive pathways through barriers appear to be absolutely necessary